Subaru Shear-and-Magnification Weak-Lensing Analysis of CLASH Galaxy Clusters

Cluster Lensing And Supernova survey with Hubble

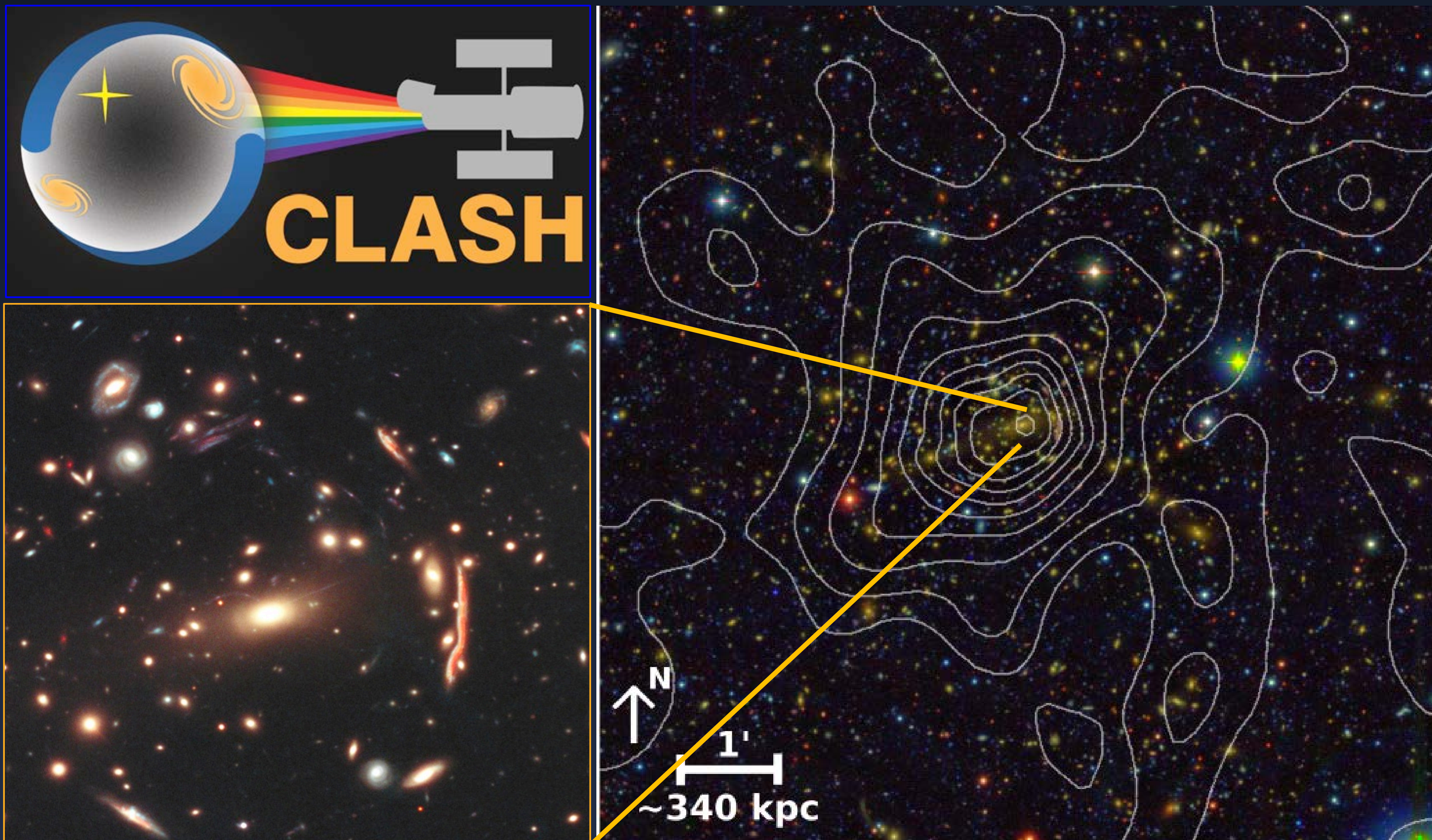

Keiichi Umetsu (ASIAA, Taiwan) with the CLASH team

Weak Lensing for Cluster Cosmology

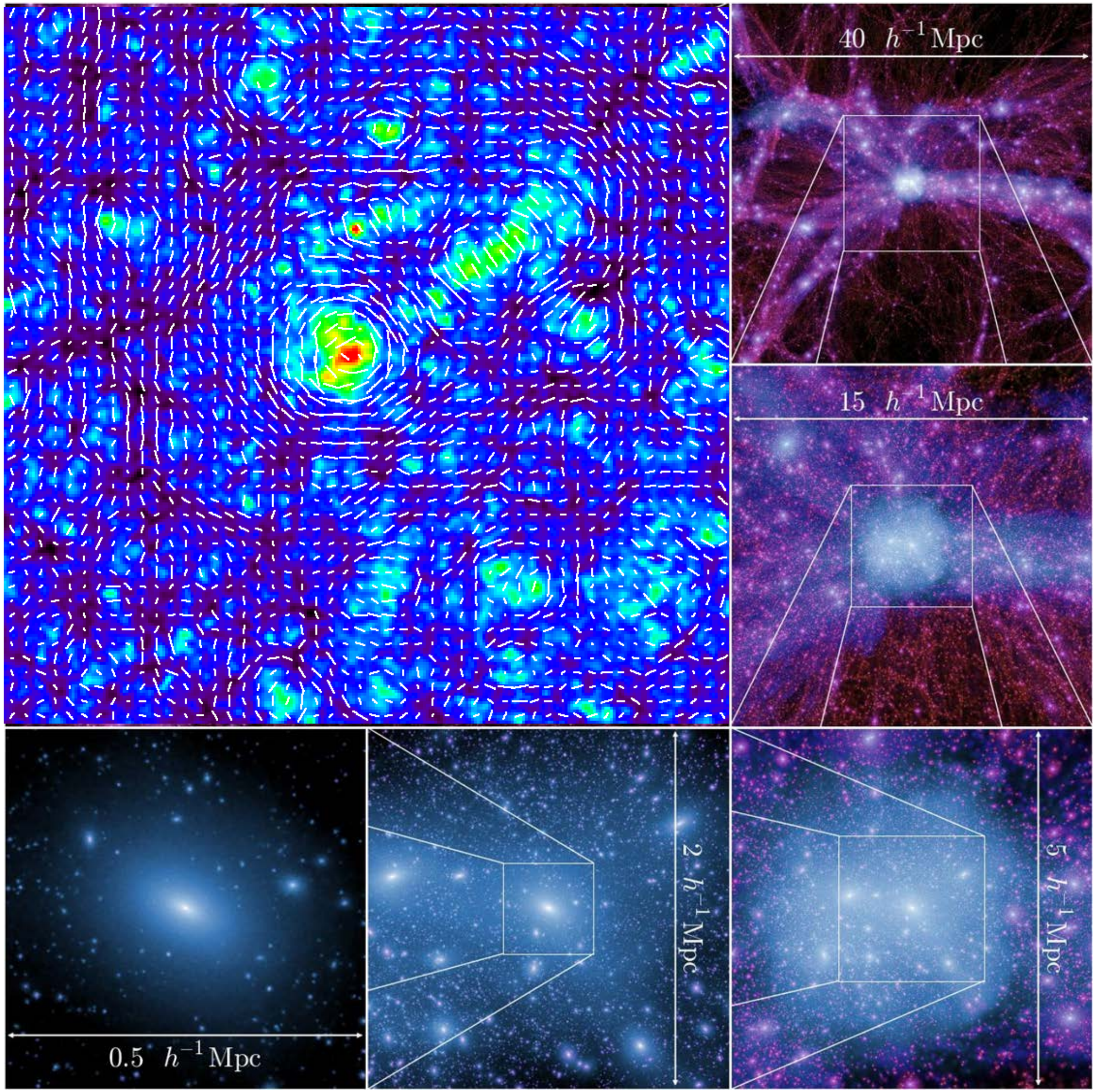

Key Ingredients

Halo structure (1h)

- Mass, M_{200c}
- Density profile, $\rho(r)$
- Concentration, $c_{200c}=r_{200c}/r_{-2}$

Surrounding LSS (2h)

- Halo bias $b(M,z)$
- Primordial matter $P(k)$

CLASH Objectives & Motivation

Before CLASH (2010), deep-multicolor Strong (*HST*) + Weak (*Subaru*) lensing data only available for a handful of "**super lens" clusters**

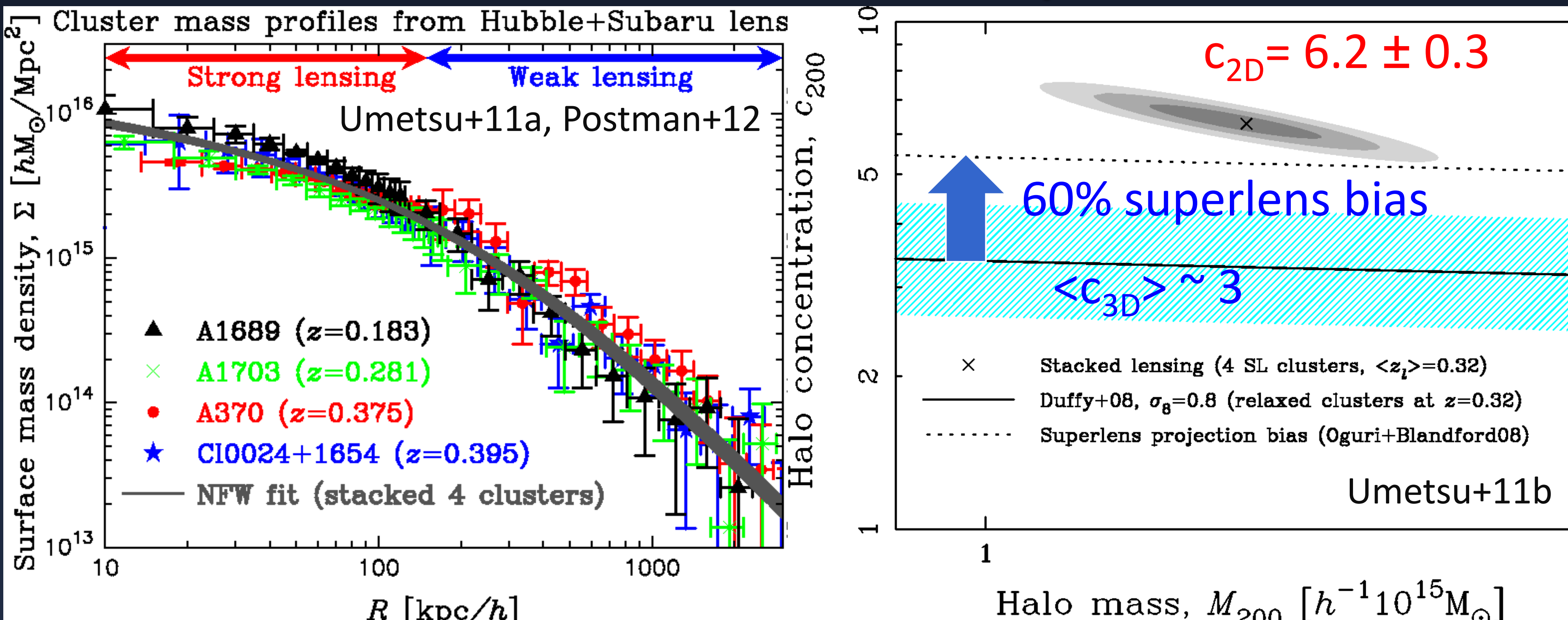

Total mass profile shape: consistent w self-similar NFW (cf. Newman+13; Okabe+13)
Degree of concentration: predicted superlens correction not enough if $\langle c_{LCDM}\rangle$~3?

CLASH Objectives & Motivation

Before CLASH (2010), deep-multicolor Strong (*HST*) + Weak (*Subaru*) lensing data only available for a handful of "**super lens" clusters**

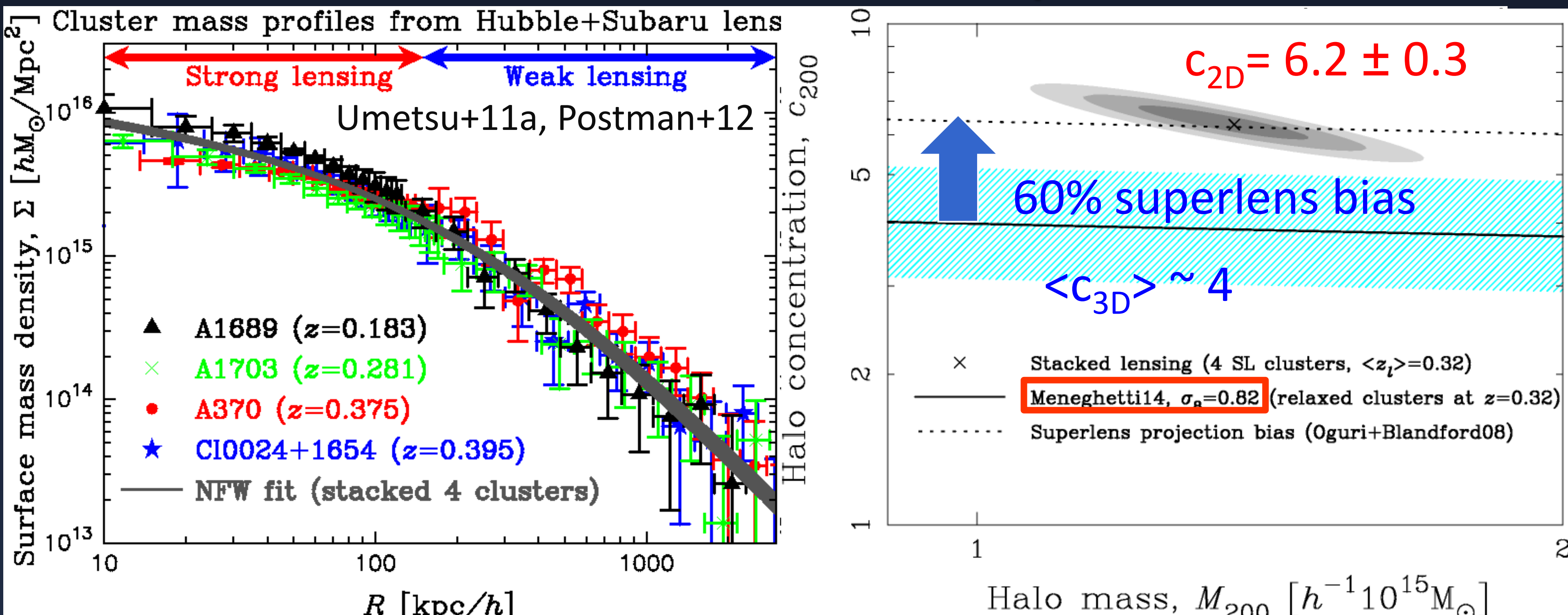

Total mass profile shape: consistent w self-similar NFW (cf. Newman+13; Okabe+13)

Degree of concentration: predicted superlens correction is just enough if $<c_{LCDM}>\sim4$

CLASH: Observational + Theory Efforts

A 524-orbit *HST* Treasury Program to observe 25 clusters in 16 filters (0.23-1.6 μm) (Postman+CLASH 12)

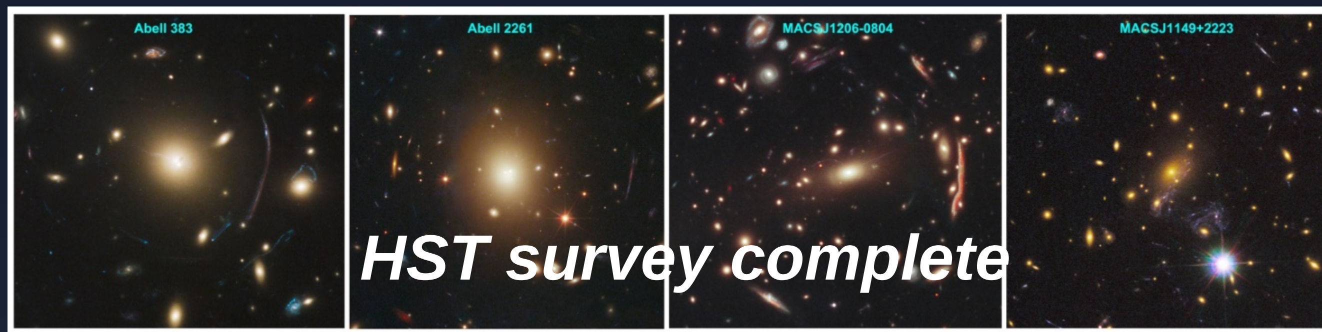

Wide-field Subaru imaging (0.4 - 0.9 μm) plays a unique role in complementing deep HST imaging of cluster cores (Umetsu et al. 2014, *ApJ*, 795, 163)

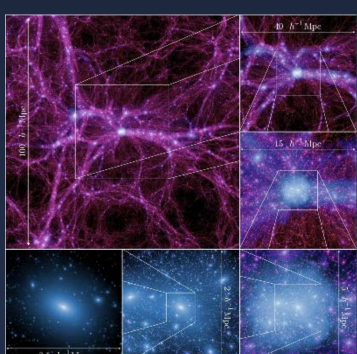

MUSIC-2 (hydro + N-body re-simulation) provides an accurate characterization of CLASH sample with testable predictions (Meneghetti+14, *ApJ*, in press; arXiv:1404.1384)

SUBARU (S-Cam) multi-color imaging for wide-field weak

High-resolution space imaging with *HST* (ACS/WFC3) for strong lensing

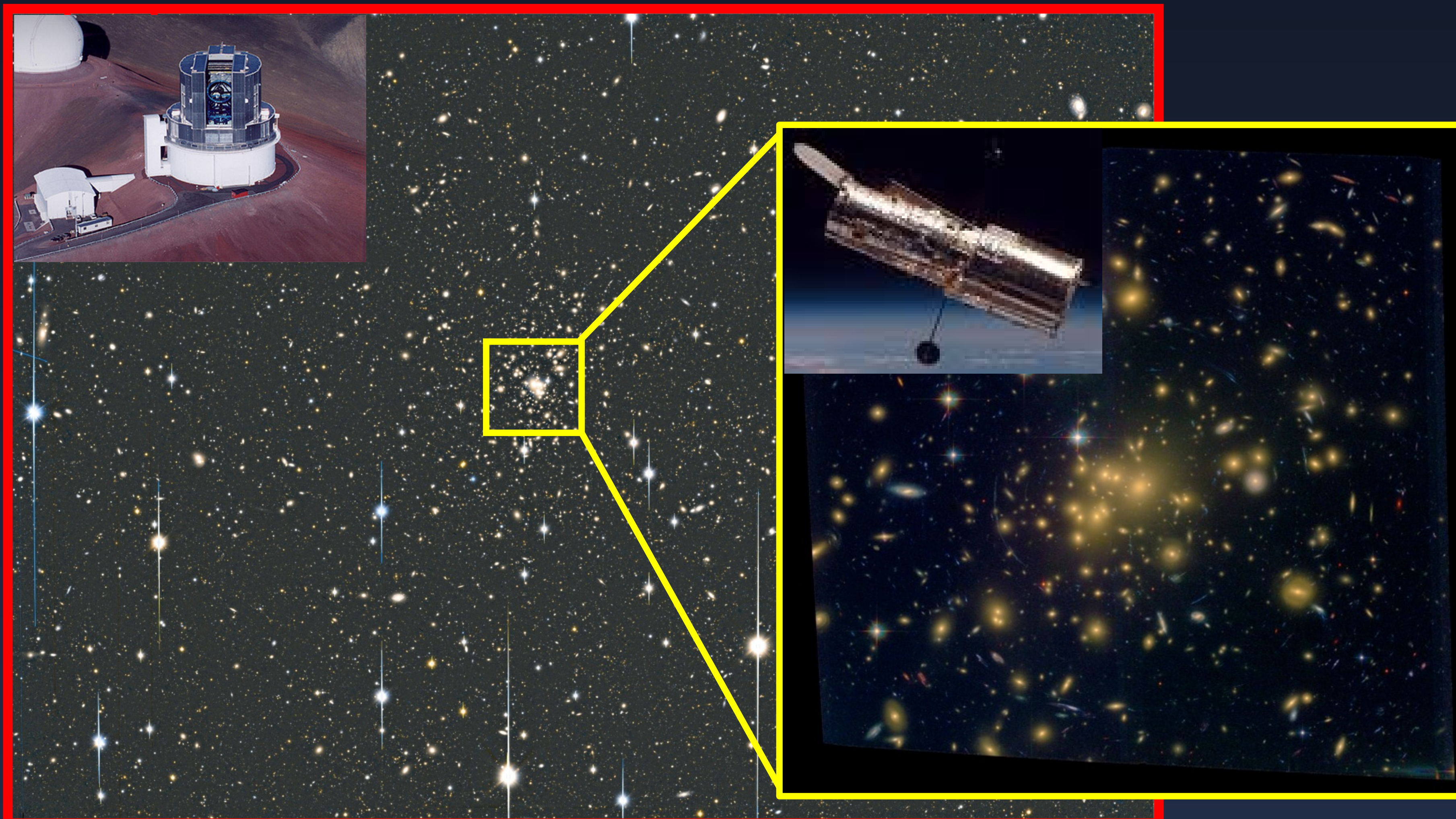

34 arcmin

CLASH X-ray-selected Subsample (0.18<z<0.9)

- **X-ray morphology + T_x selection**
  - $T_x > 5$keV ($M_{200c} > 5e14 M_{sun}/h$)
  - Small BCG to X-ray-peak offset, σ_{off} ~ 10kpc/h
  - Smooth regular X-ray morphology

→ Optimized for radial-profile analysis ($R > 2\sigma_{off}$ ~ 20kpc/h)

- **CLASH theoretical predictions** (Meneghetti+CLASH 14)
  - Composite relaxed (70%) and unrelaxed (30%) clusters
  - Mean $\langle c_{200c} \rangle = 3.9$, $\sigma(c_{200c}) = 0.6$, $c_{200c} = [3, 6]$
  - Negligible orientation bias (~2% in $\langle M_{3D} \rangle$)
  - >90% of CLASH clusters to have strong-lensing features

Shear and Magnification Effects

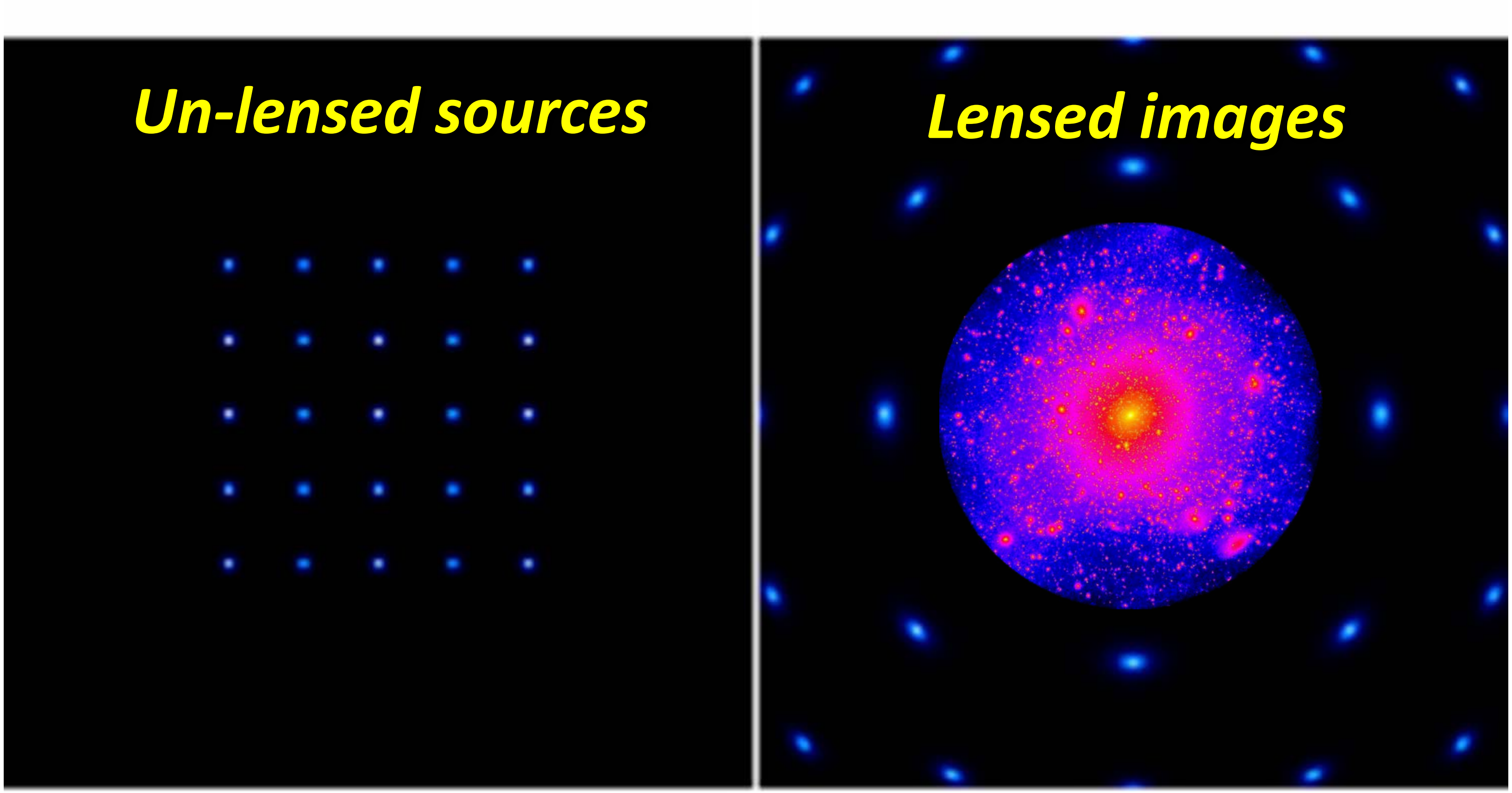

- **Shear**
  - ✓ Geometric shape dist.: $\delta e_+ \sim \gamma_+$

Sensitive to "modulated" matter density

$$\Sigma_{\rm crit}\gamma_+ = \Delta\Sigma(R) \equiv \Sigma(<R) - \Sigma(R)$$

- **Magnification**
  - ✓ Flux amplification: μF
  - ✓ Geometric area dist.: $\mu\Delta\Omega$

Sensitive to "total" matter density

$$\mu \approx 1 + 2\kappa; \quad \Sigma_{\rm crit}\kappa = \Sigma(R)$$

Shear doesn't see mass sheet

Averaged lensing profiles in/around LCDM halos (Oguri+Hamana 11)

Total

$$\kappa = \Sigma(R)/\Sigma_{\rm crit}$$

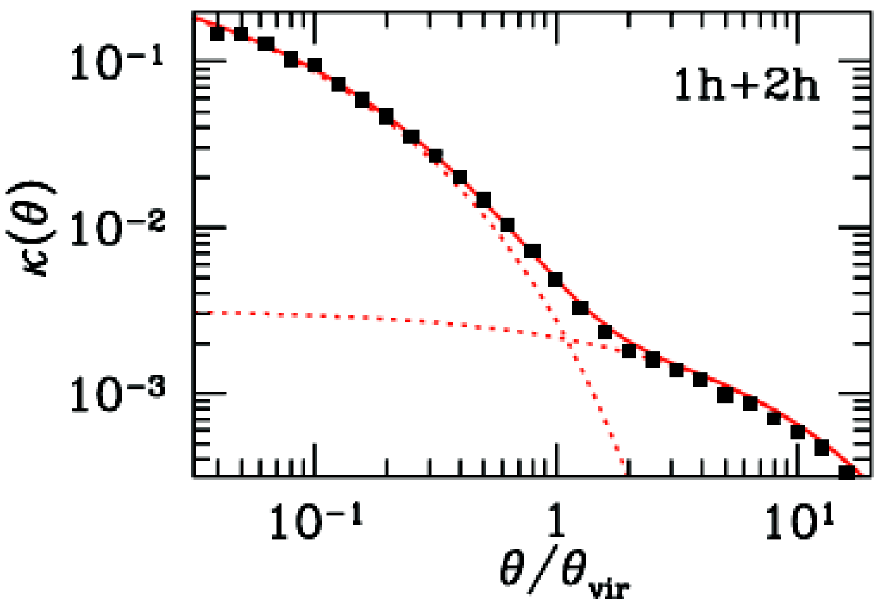

Modulated

$$\gamma_+ = \Delta\Sigma(R)/\Sigma_{\rm crit}$$

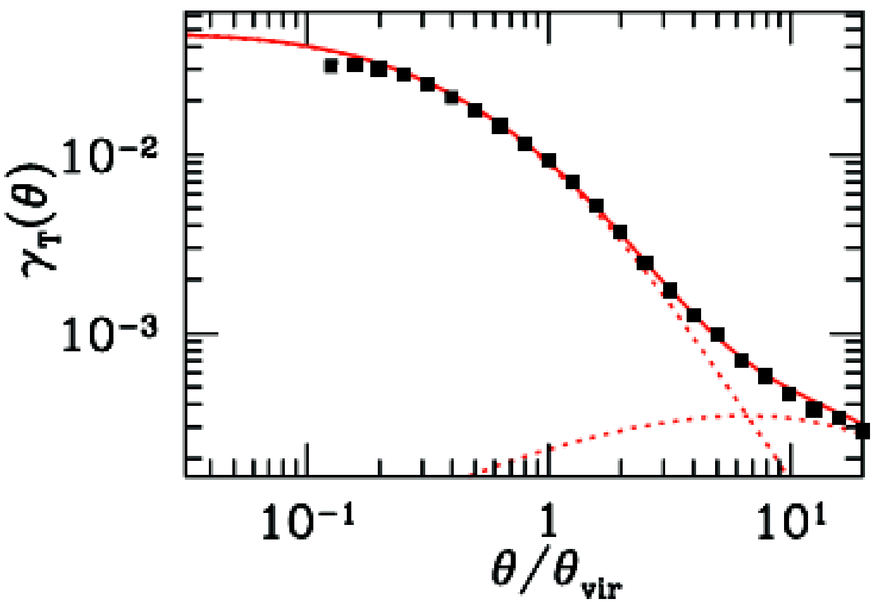

- **Tangential shear is a powerful probe of 1-halo term, or internal halo structure.**
- **Shear alone cannot recover absolute mass, known as *mass-sheet degeneracy:***

γ remains unchanged by $\kappa \to \kappa + \text{const.}$

CLASH Weak-Lensing Results (1)

Ensemble-averaged dark-matter halo structure:

- Cluster halo density profile, $<\Delta\Sigma(R)>$
- Degree of mass concentration, $<c_{200c}>$

from ***stacked-shear-only WL*** analysis

of 16 CLASH X-ray-selected clusters

Umetsu+CLASH 2014, *ApJ*, 795, 163 (arXiv:1404.1375)

Averaged Halo (1h) Density Profile

Stacking of WL-shear signals by weighting individual clusters according to the sensitivity kernel matrix:

$$\langle\langle \widehat{\Delta\Sigma_+} \rangle\rangle = \left(\sum_n \mathcal{W}_{+n} \right)^{-1} \left(\sum_n \mathcal{W}_{+n} \widehat{\Delta\Sigma_{+n}} \right),$$

Summing over clusters (n=1, 2, ..)

with individual sensitivity matrix

$$(\mathcal{W}_{+n})_{ij} \equiv \Sigma_{c,n}^{-2} \left(C_{+n}^{-1} \right)_{ij}$$

defined with total covariance matrix

$$C_+ = C_+^{\rm stat} + C_+^{\rm sys} + C_+^{\rm lss}.$$

With "trace-approximation", averaging (stacking) is interpreted as

$$\langle\langle \Sigma_c^{-1} \rangle\rangle = \frac{\sum_n \mathrm{tr}(\mathcal{W}_{+n}) \Sigma_{c,n}^{-1}}{\sum_n \mathrm{tr}(\mathcal{W}_{+n})},$$

Umetsu et al. 2014, *ApJ*, 795, 163

Stacked Halo Density Profile $\Delta\Sigma(R)$

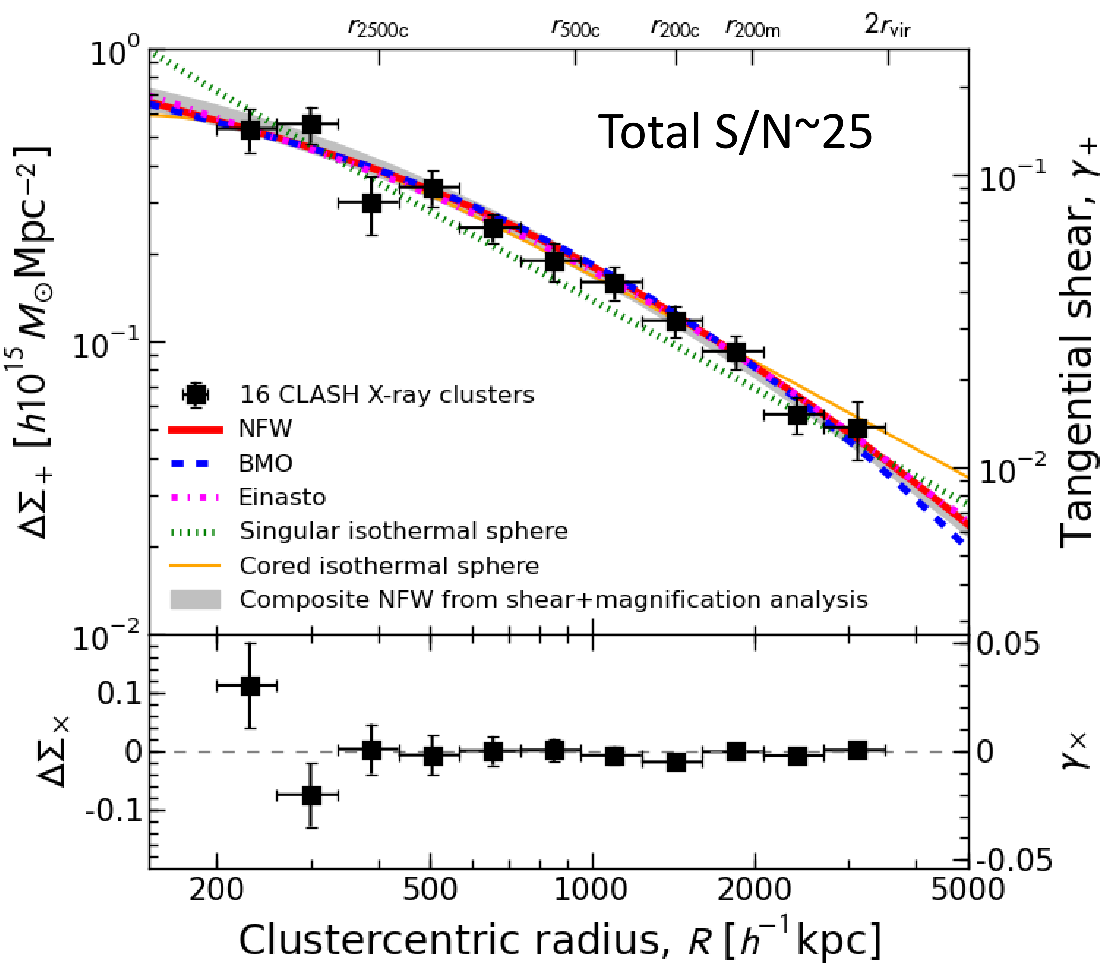

Stacked-shear-only analysis provides a net 1-halo-only constraint ($\gamma_{+,2h}<10^{-3}$) at <z>=0.35

NFW an excellent fit (PTE = 0.66)

- M_{200c} = (1.3+/-0.1) $10^{15} M_{sun}$
- c_{200c} = 4.01 (+0.35, -0.32)

Einasto model (PTE=0.51)

- Einasto shape parameter α=0.19+/-0.07, consistent with NFW profile curvature (α~0.18)

Umetsu+CLASH 14, *ApJ*, 795, 163

Consistent w a family of density profiles for collisionless DM halos (NFW, truncated variants of NFW, Einasto)

Integrated Constraints on $c(M_{200c},z)$

Theoretical predictions for stacked $c(M,z)$

$$\langle c_{200c} \rangle = \frac{\int dM dz N(M,z) \hat{c}_{200c}(M,z)}{\int dM dz N(M,z)} \approx \frac{\sum_n \mathrm{tr}(\mathcal{W}_n) \hat{c}_{200c}(M_n, z_n)}{\sum_n \mathrm{tr}(\mathcal{W}_n)}$$

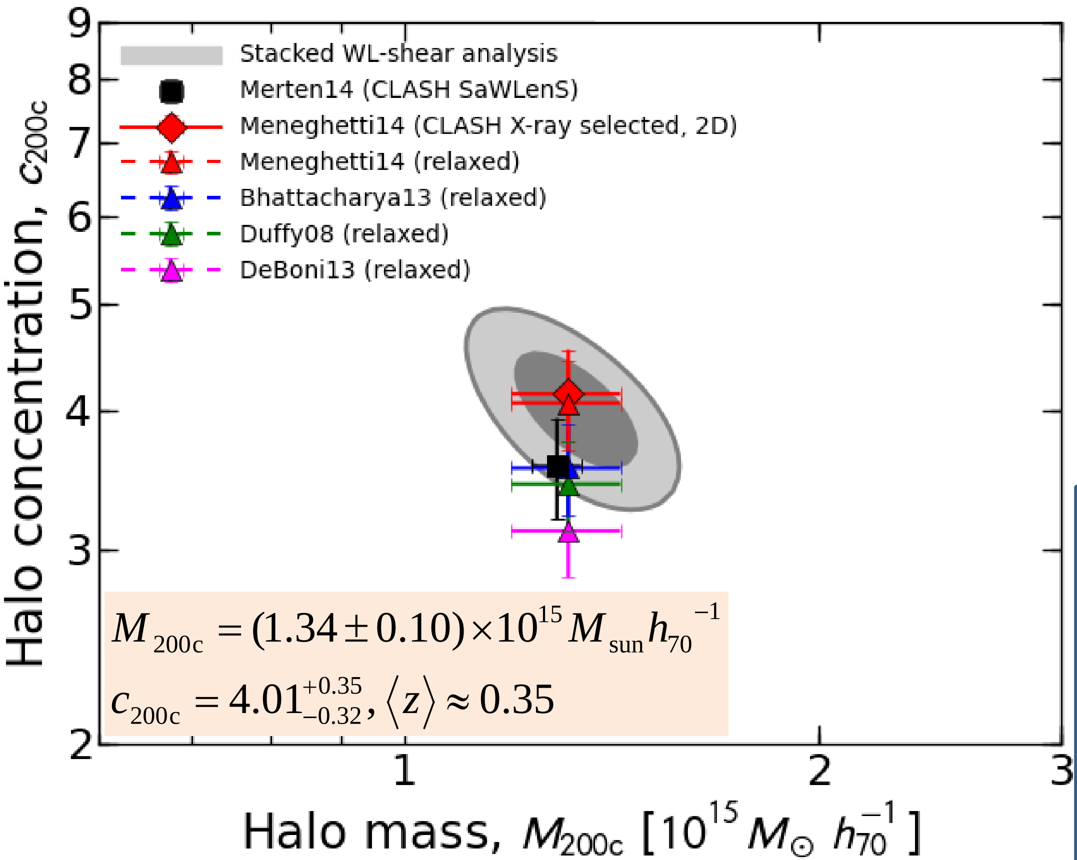

Variance in theory due primarily to different cosmology (σ_8)

Meneghetti14: σ_8=0.82

Bhattacharya13: σ_8=0.8

Duffy08: σ_8=0.796

DeBoni13: σ_8=0.776

- Excellent agreement with CLASH predictions (M14), c_{200c} ~ 4.0
- Consistent with Bhatt13, Duffy08 predictions for "relaxed" halos at 1σ, c_{200c}~3.6

Umetsu+CLASH 14, *ApJ*, 795, 163

CLASH Weak-Lensing Results (2)

Individual cluster mass properties:

- Cluster mass profiles $\Sigma(R)$ from **joint *shear* + *magnification* WL analysis**
- Cluster mass estimates (M_{500c}, M_{200c}, M_{vir}, M_{200m}) assuming spherical NFW profiles

of 20 CLASH Clusters

Umetsu+CLASH 2014, *ApJ*, 795, 163 (arXiv:1404.1375)

Combining Shear and Magnification

Bayesian joint likelihood approach (Umetsu+11a; Umetsu 13)

Tangential (reduced) shear $$g_+(R) = \frac{\kappa(<R) - \kappa(R)}{1 - \kappa(R)},$$

Inverse magnification $$\mu^{-1}(R) = [1 - \kappa(R)]^2 - [\kappa(<R) - \kappa(R)]^2$$

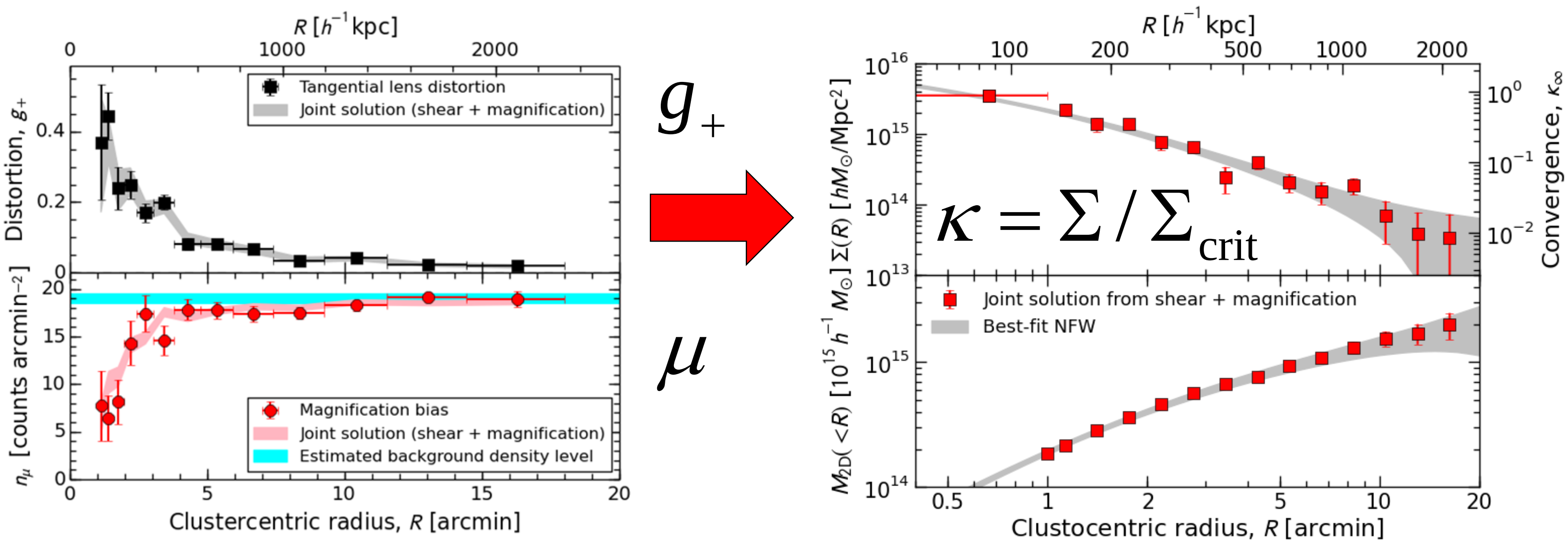

- Mass-sheet degeneracy broken
- Total statistical precision improved by ~20-30%
- Calibration uncertainties marginalized over: $c = \{\langle W \rangle_s, f_{W,s}, \langle W \rangle_\mu, \bar{n}_\mu, s_{\rm eff}\}.$

Joint Shear + Magnification WL Analysis

CLASH low mass

M_{200c}=6e14Msun/h (z=0.19)

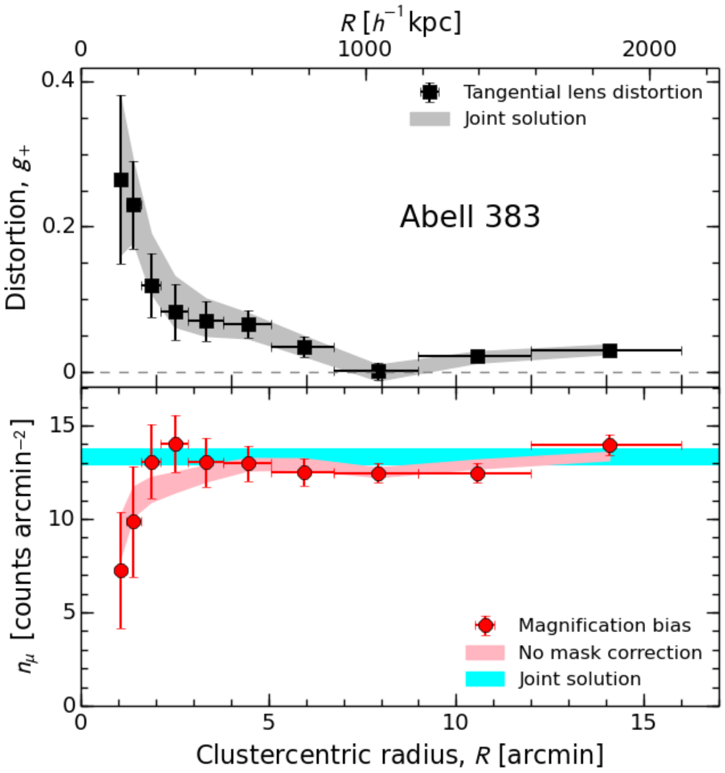

CLASH high mass

M_{200c}=20e14Msun/h (z=0.45)

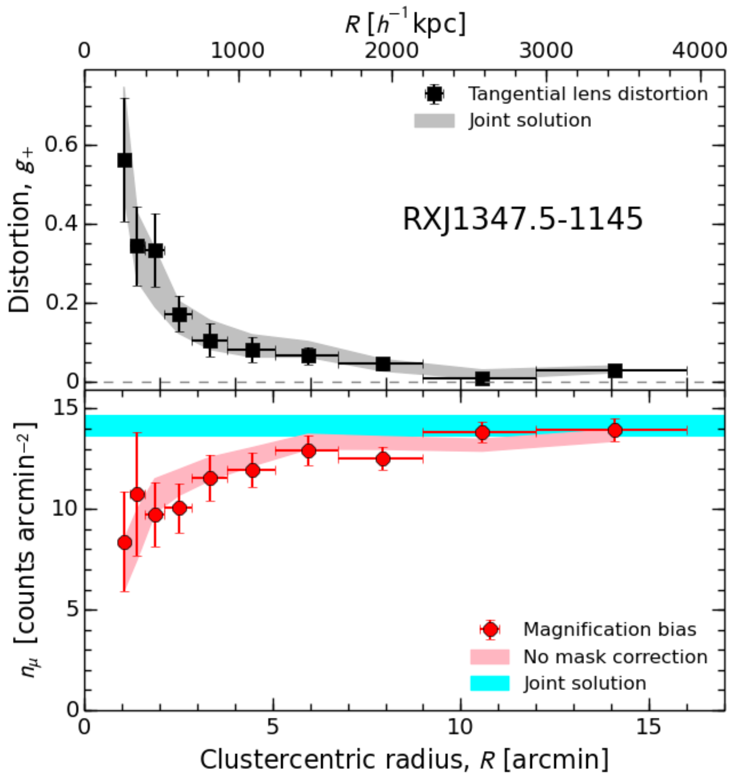

Shear-magnification consistency: $<\chi^2/\mathrm{dof}> = 0.92$ for 20 CLASH clusters

Systematic mass calibration uncertainty $\sigma_{M,3D} < 8\%$

CLASH Mass Density Profile Dataset

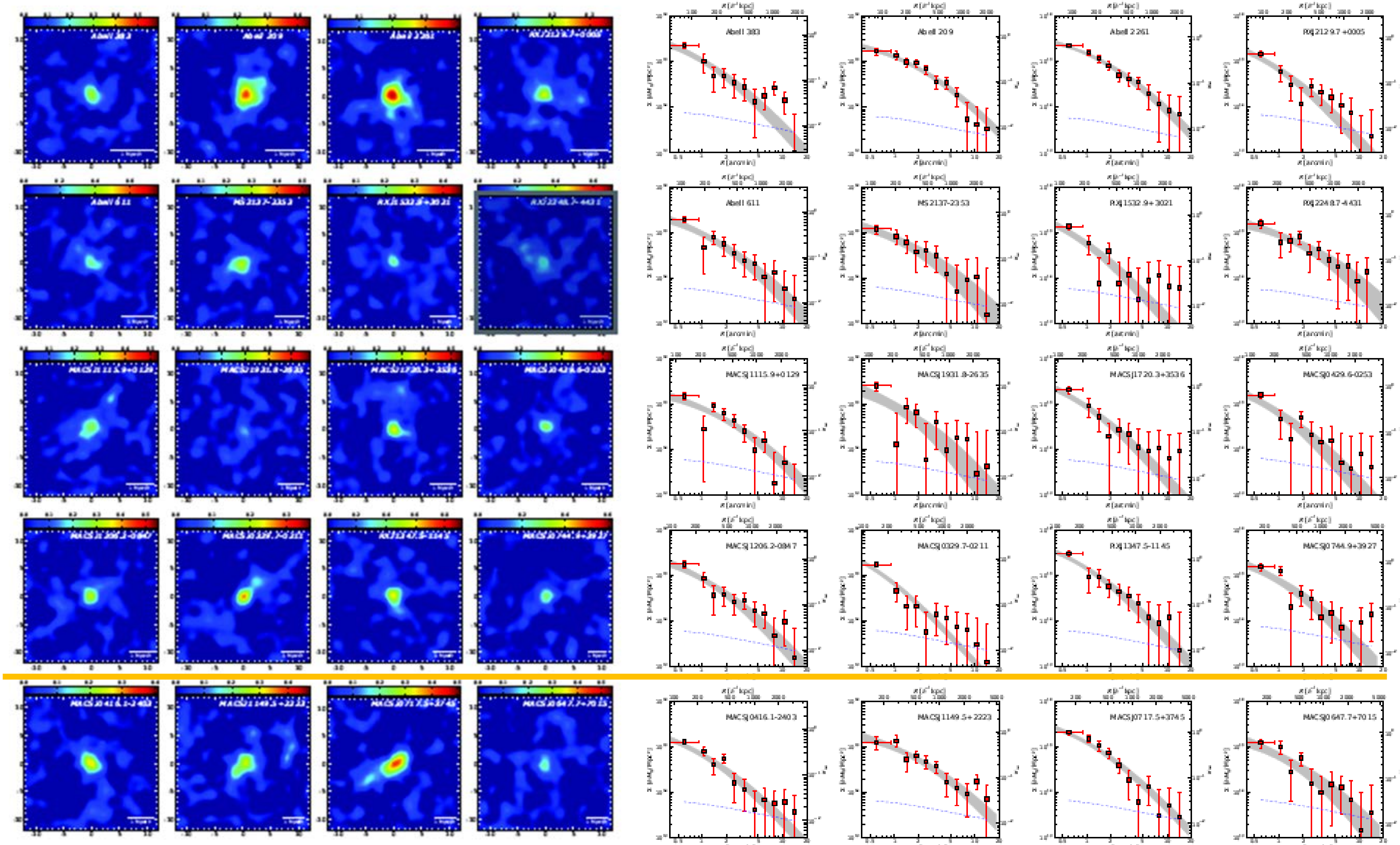

Umetsu+CLASH 2014, *ApJ*, 795, 163 (arXiv:1404.1375)

Comparison with *Planck* Masses

Mass-dependent bias (20-45%) observed for *Planck* mass estimates

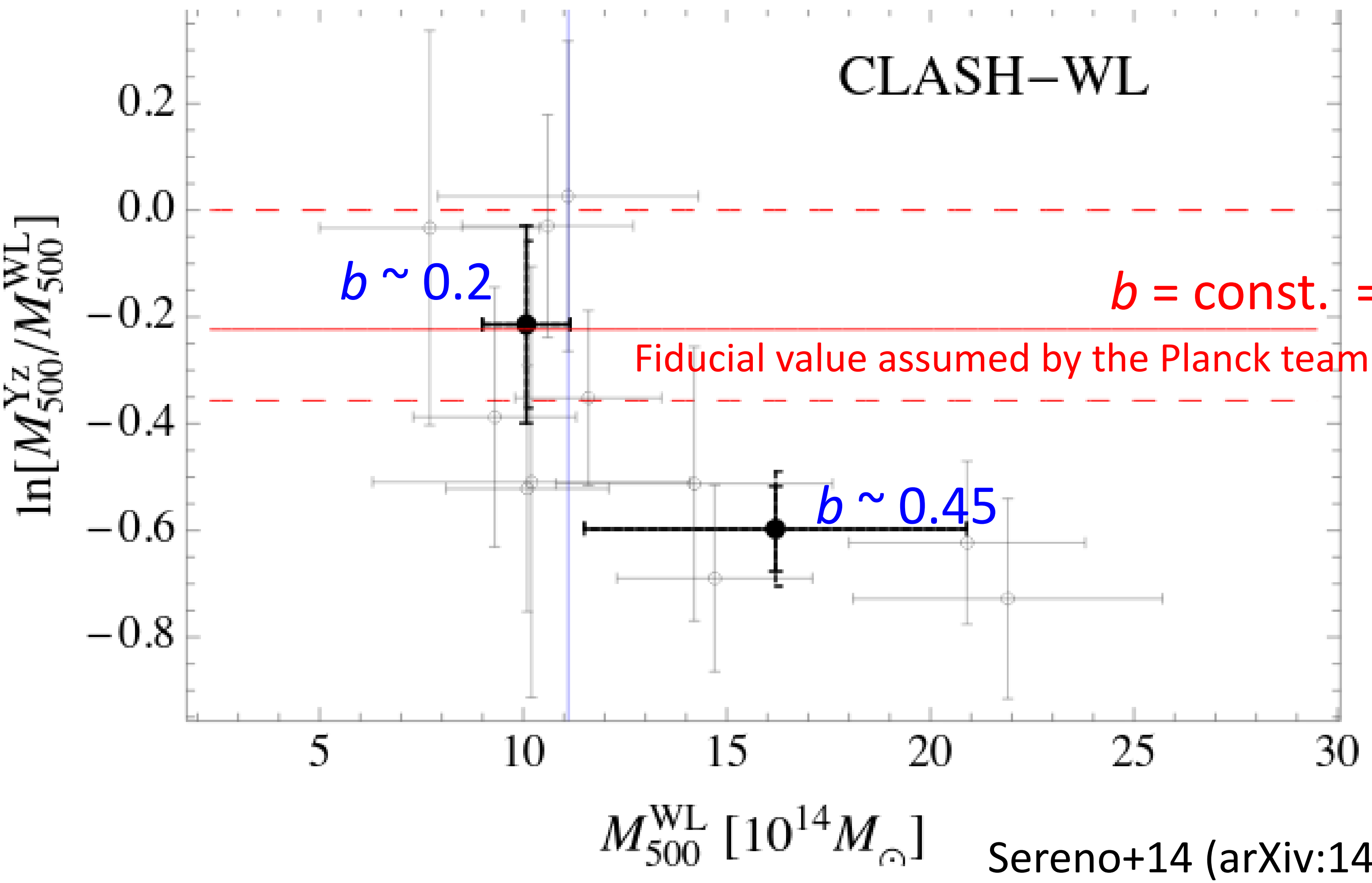

Sereno+14 (arXiv:1407.7869)

CLASH: Strong-lensing, Weak-lensing Shear and Magnification

- Mass profile reconstruction from **full likelihood analysis of *Strong-Lensing, Weak-Lensing shear and magnification*** constraints (Umetsu13 multi-probe method)

$$L(\boldsymbol{\kappa}) = L_g(\boldsymbol{\kappa} \mid g_+) L_\mu(\boldsymbol{\kappa} \mid \mu^{\alpha-1}) L_{\mathrm{SL}}(\boldsymbol{\kappa} \mid M_{\mathrm{2D}})$$

1. Stacked mass profile analysis $\langle\Sigma(R)\rangle$ at $R=[0.01,2]r_{\mathrm{vir}}$

1h term **2h term**

$$\Sigma_{\mathrm{tot}}(R \mid M) = \Sigma_{\mathrm{1h}}(R \mid M) + b_{\mathrm{h}}(M)\Sigma_{\mathrm{m}}(R)$$

2. Concentration-mass-redshift relation $c_{200c}(M_{200c},z)$

Umetsu+CLASH 2015, in prep

Averaged Total Mass Profile

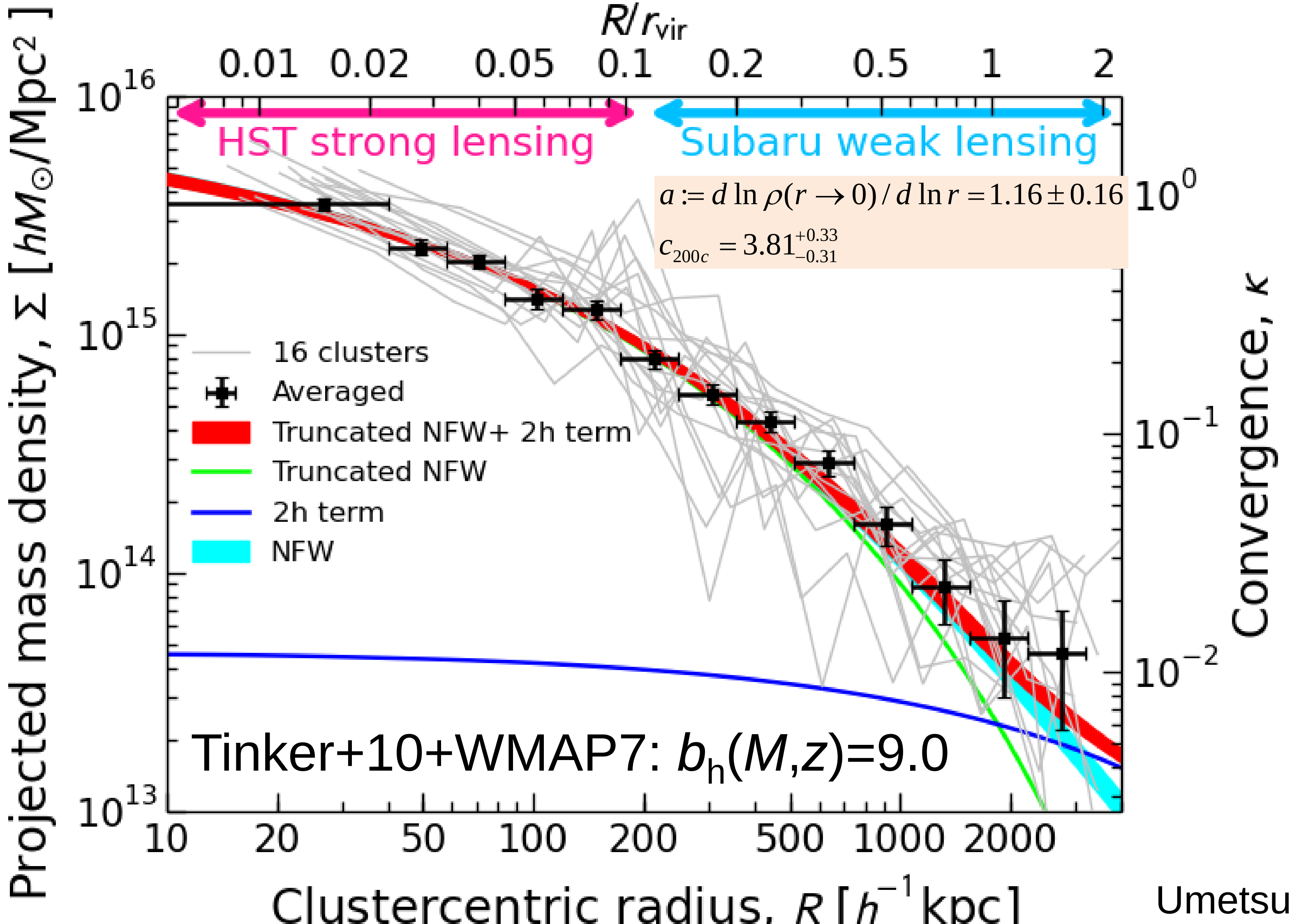

Umetsu+2015, in prep

Averaged Total Mass Profile

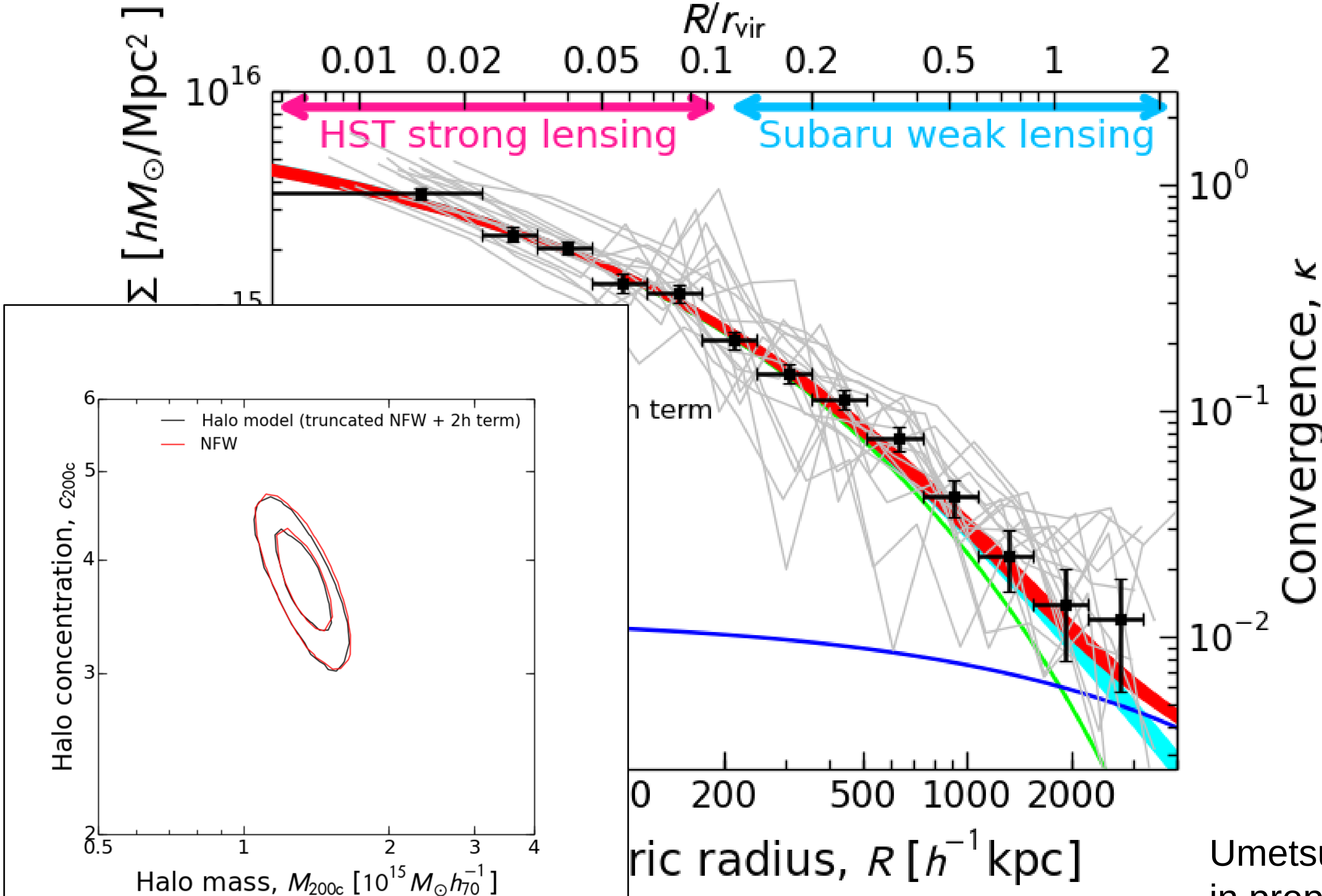

Umetsu+2015, in prep

C-M relation

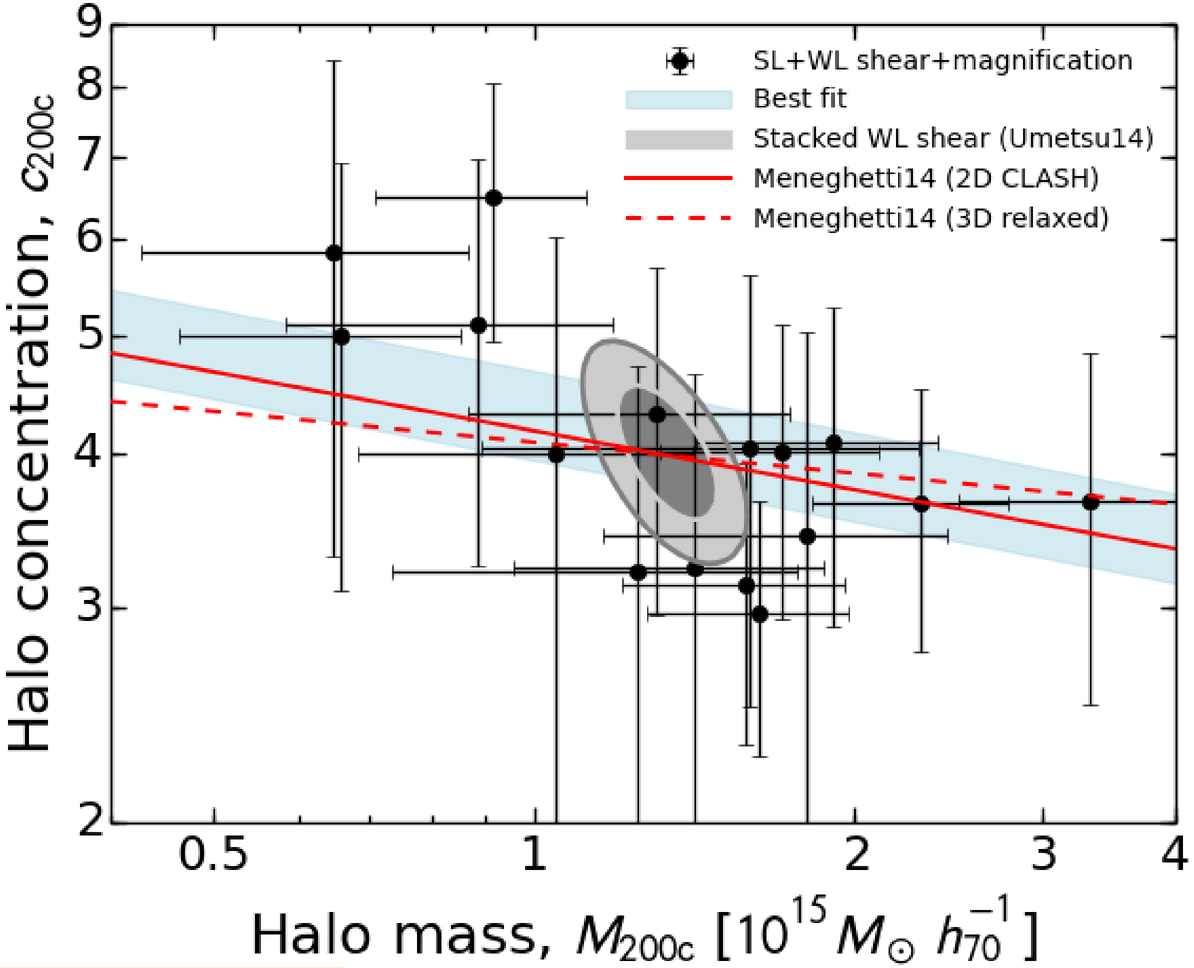

$\partial \ln c / \partial \ln M = -0.16 \pm 0.08$

$c(9 \times 10^{14} M_{sun}, z = 0.35) = 4.10 \pm 0.35$

$\sigma_{\ln c} < 0.1$

Umetsu+2015, in prep

Summary

- Observed c-M relation is consistent with
  - theoretical expectation (σ_8=0.82), $\langle c_{200c} \rangle \sim 3.9$, which accounts for CLASH selection function and projection effects
- Consistent shear-magnification measurements allow for accurate cluster mass profile measurements for 20 CLASH clusters with +/-8% systematic mass-calibration uncertainty.
- Averaged total matter distribution $\langle \Sigma \rangle$ at R=[0.01,2]r_{vir} from full-lensing analysis (SL + shear + magnification) is consistent with LCDM halo-model with c_{200c}=4.0+/-0.3, M_{200c}=(1.3+/-0.1)$10^{15} M_{sun}$, $b_h \sim 9$

CLASH Products released

http://archive.stsci.edu/prepds/clash/

- Calibrated and co-added images [HST, Subaru]
- Object catalogs [HST, Subaru]

Subaru (S-Cam) product release will be completed by September 2014

CLASH-WL Summary

- Ensemble-averaged halo structure $\Delta\Sigma$ (1h) of X-ray-regular CLASH clusters is consistent with a family of standard (collisionless) DM predictions:
  - M_{200c}= (1.3 +/- 0.1) $10^{15} M_{sun}$, <z>=0.35
  - NFW (PTE=0.66): c_{200c}=4.01 (+0.35, -0.32)
  - Einasto (PTE=0.51): degree of curvature, α_E=0.19 +/- 0.07
- The stacked-mean concentration agrees with:
  - theoretical expectation, $\langle c_{200c} \rangle \sim 3.9$, which takes into account CLASH selection function and projection effects (Meneghetti+14)
  - measured effective Einstein radius, $\langle \theta_{Ein} \rangle$=20” ($z_s$=2), from independent HST-SL analysis (Zitrin+CLASH 14, in prep)

CLASH-WL Summary (contd.)

- Consistent geometric shear vs. magnification measurements allow for accurate cluster mass profile measurements for 20 CLASH clusters with +/-8% systematic mass-calibration uncertainty.
- Total matter distribution Σ (1h+2h) recovered from full-lensing analysis (SL + shear + magnification) is consistent with shear-based halo model predictions (b_h=9+/2 at M_{200}=1.3e15M_{sun}, z=0.35), establishing further consistency in the context of LCDM.

Supplemental Slides

Latest simulation vs. CLASH

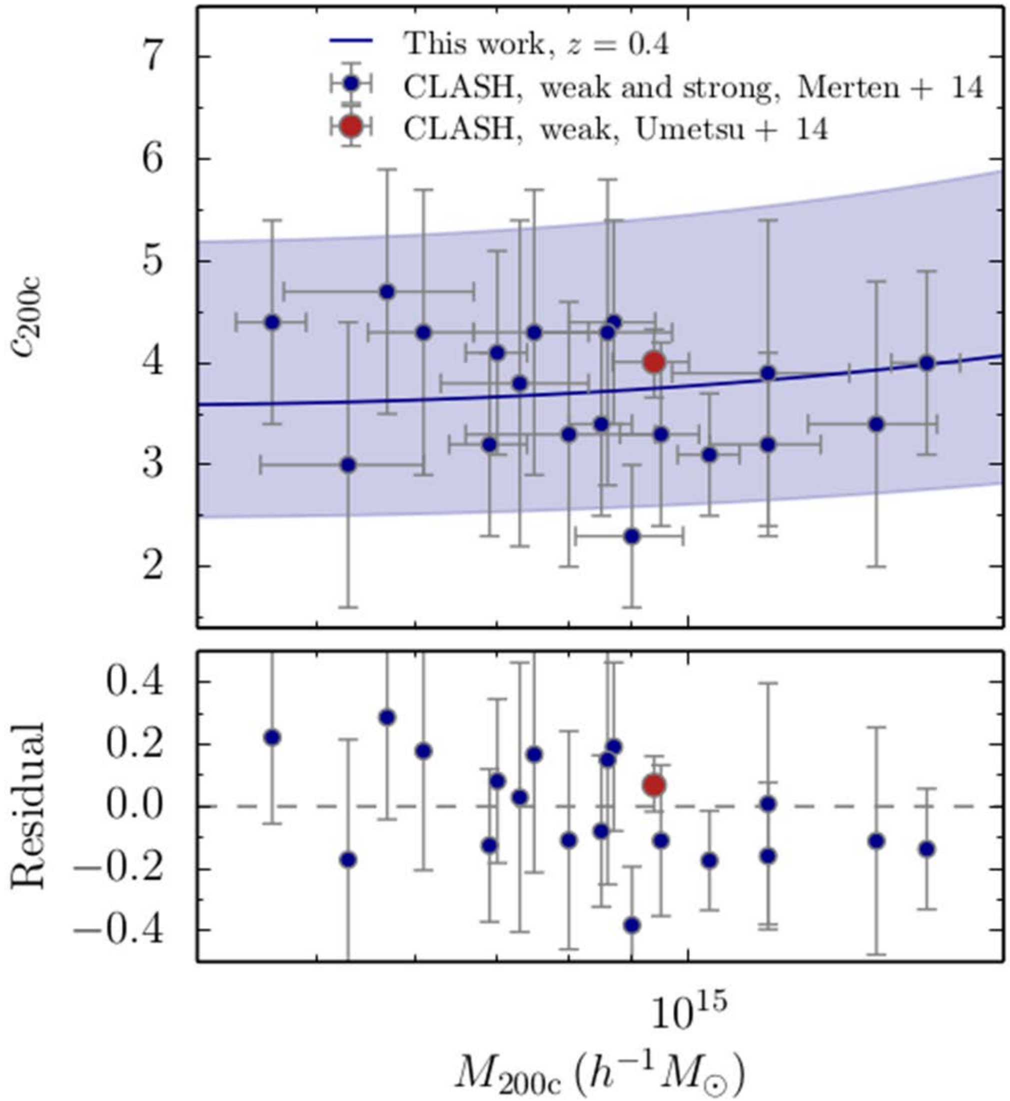

Figure from Diemer & Kravtsov 2014b

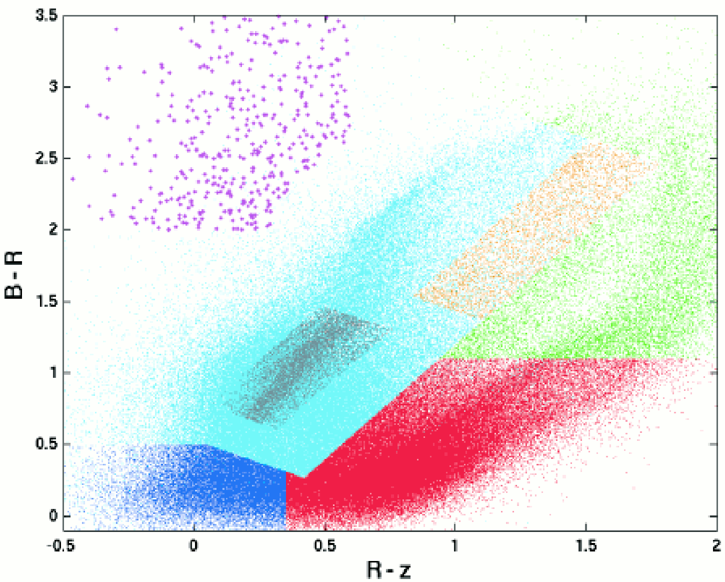
B - R
R - z

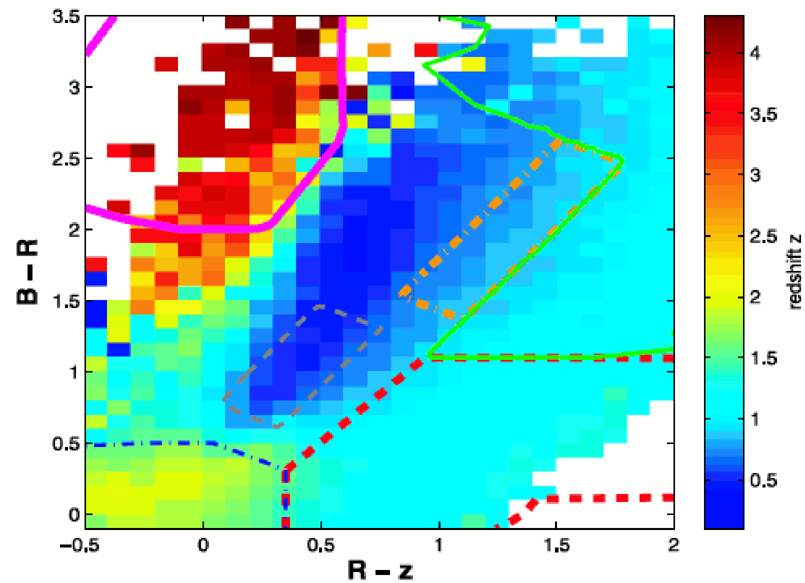
B – R
R – z
redshift z

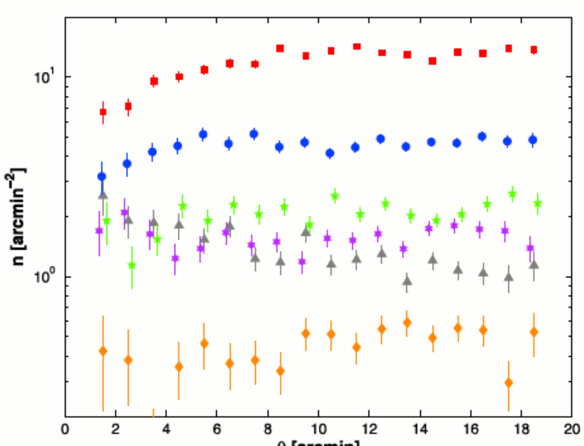
n [arcmin^{-2}]
θ [arcmin]

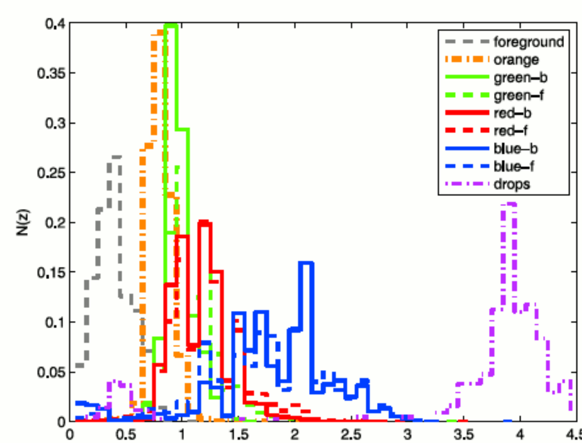
N(z)
z
foreground
orange
green–b
green–f
red–b
red–f
blue–b
blue–f
drops

SUBARU shear strength as a function of magnitude

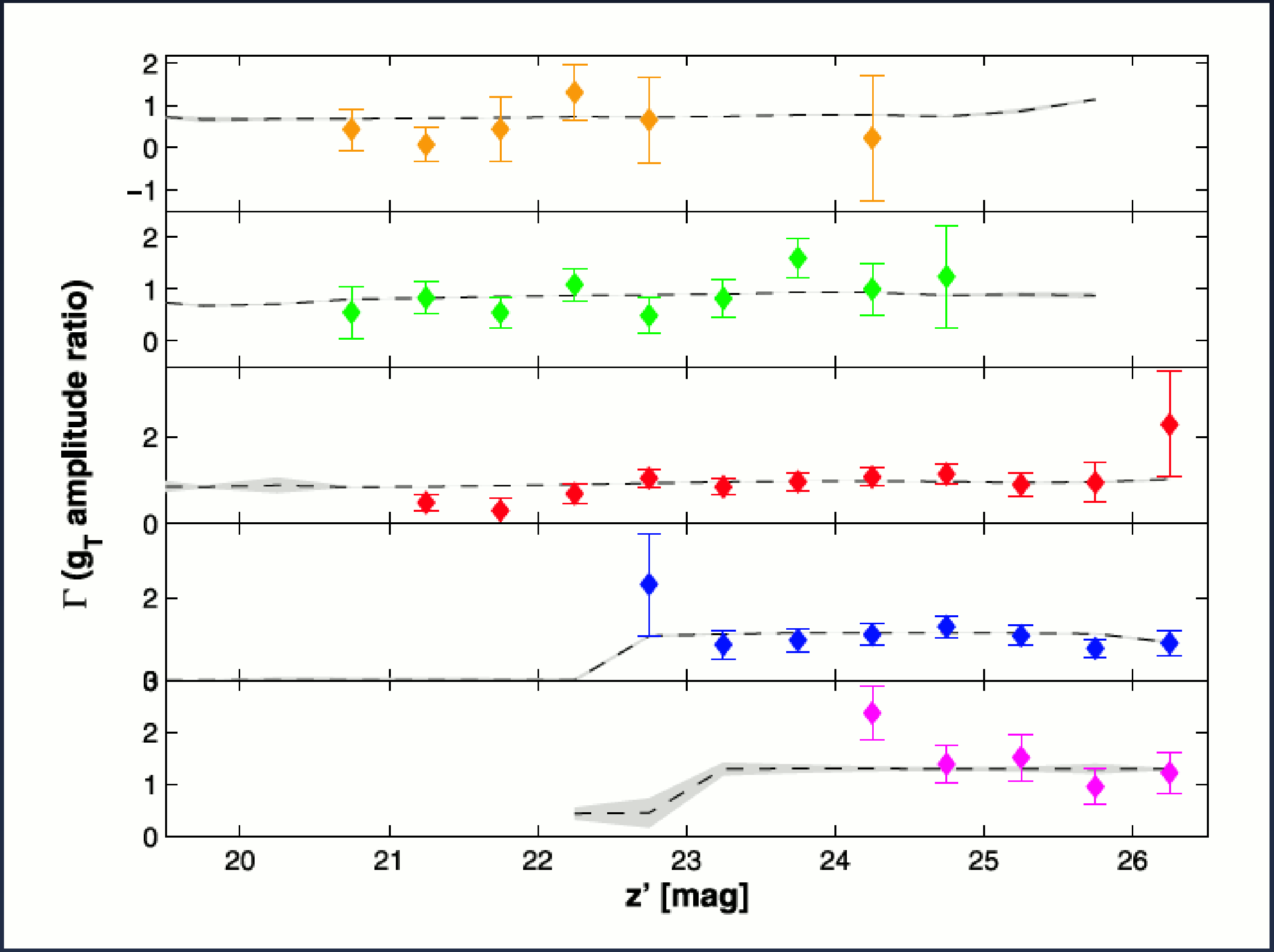

Medezinski, Broadhurst, Umetsu+11

Non-local substructure effect

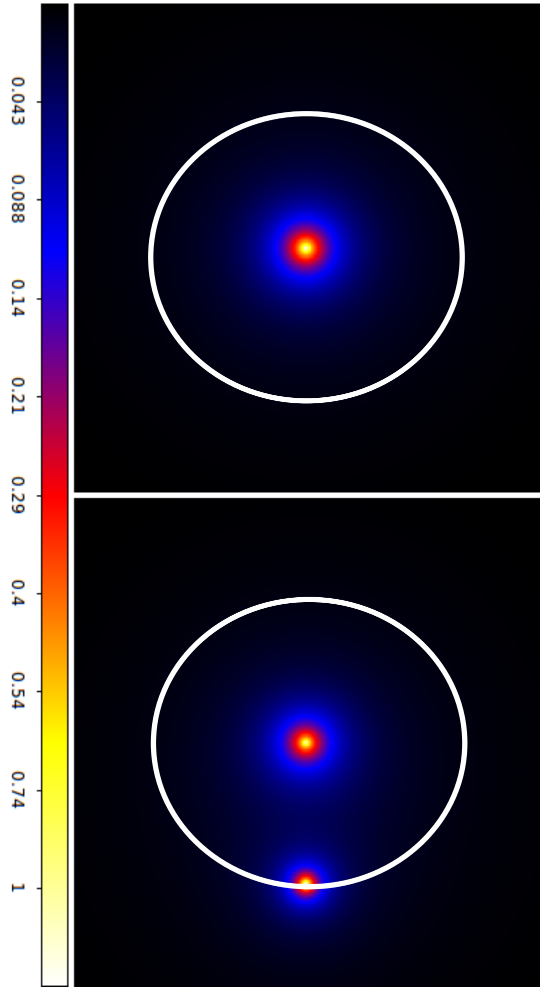

A substructure at R ~ r_{vir} of the main halo, modulating $\Delta\Sigma(R) = \Sigma(< R) - \Sigma(R)$

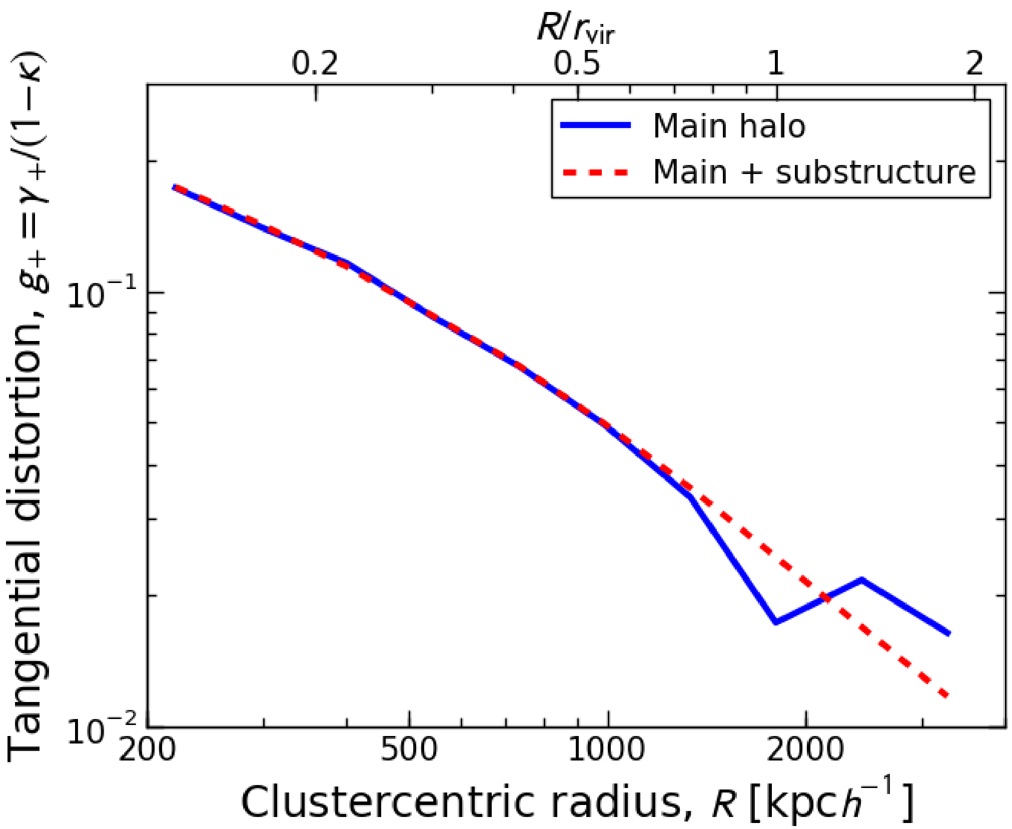

Known ~10% negative bias in mass estimates from tangential-shear fitting, inherent to clusters sitting in substructured field (Rasia+12)

Magnification bias effects

Flux-limited source counts:

$$n_{\mathrm{obs}}(>f) = \mu^{-1} n(>\mu^{-1} f)$$

Broadhurst, Taylor & Peacock 95

Geometric area distortion

n/μ

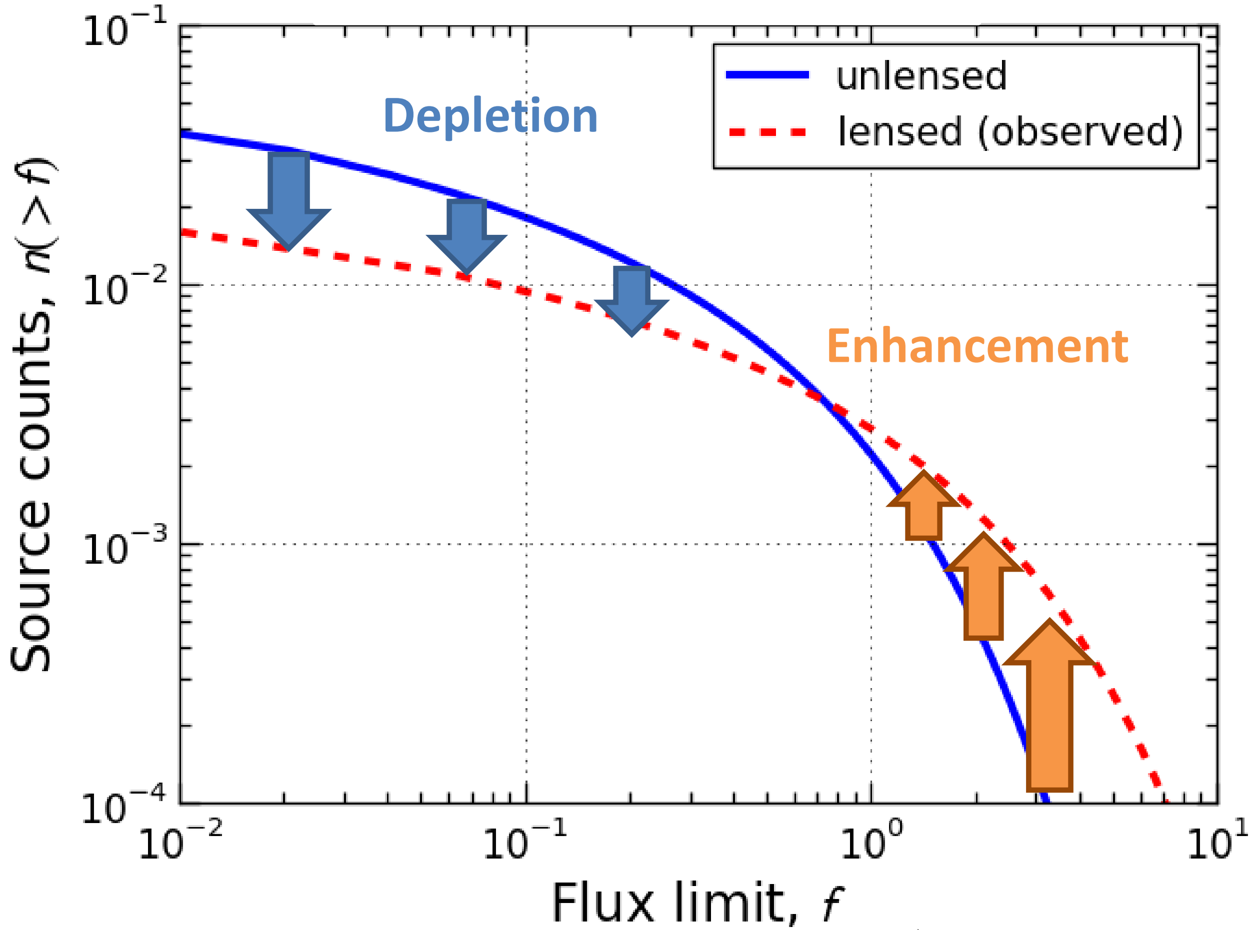

Flux amplification

Cluster masses recovered from lensing analysis

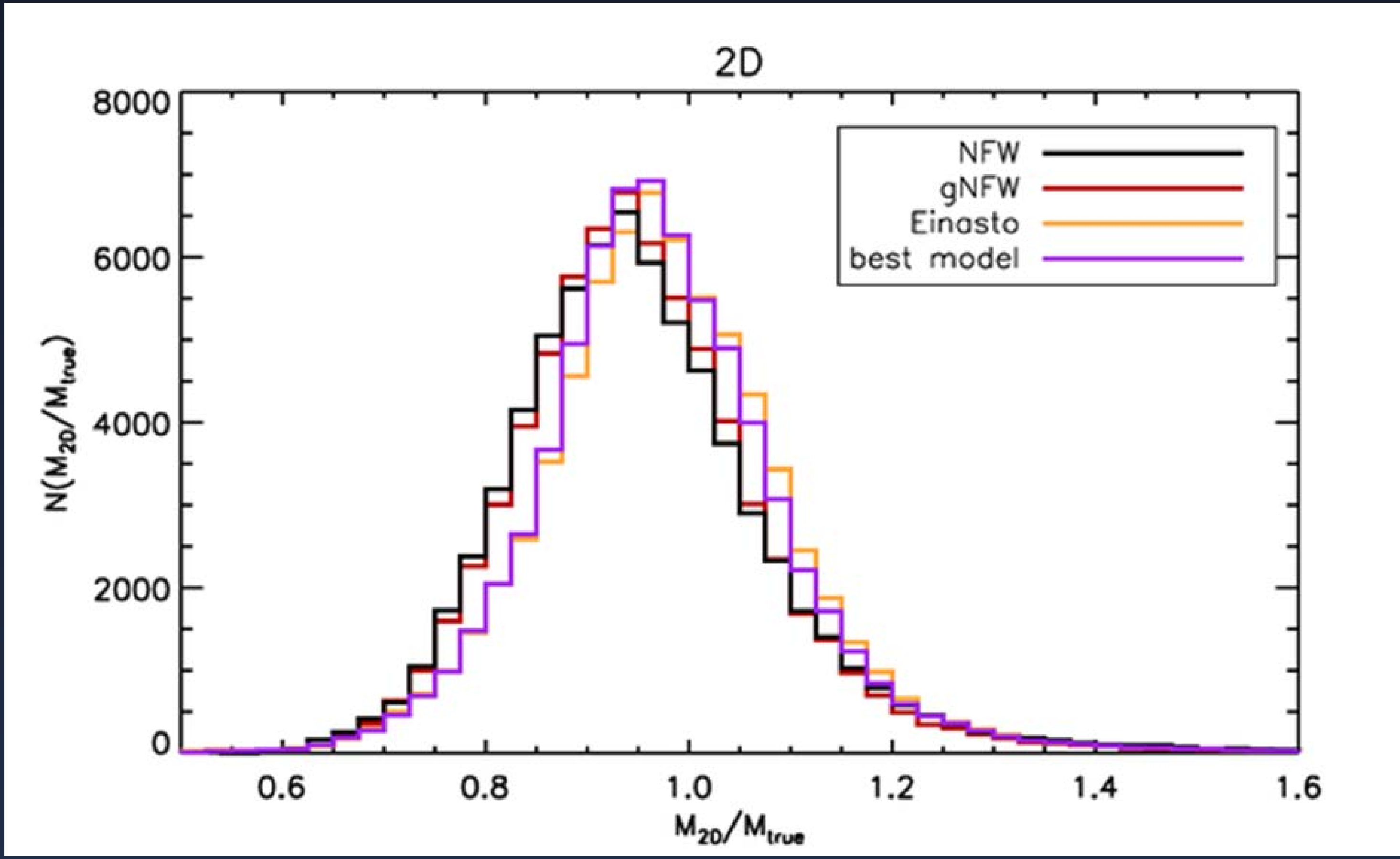

Meneghetti+CLASH 14

Scatter in $M_{2D}(R)$ by halo triaxiality

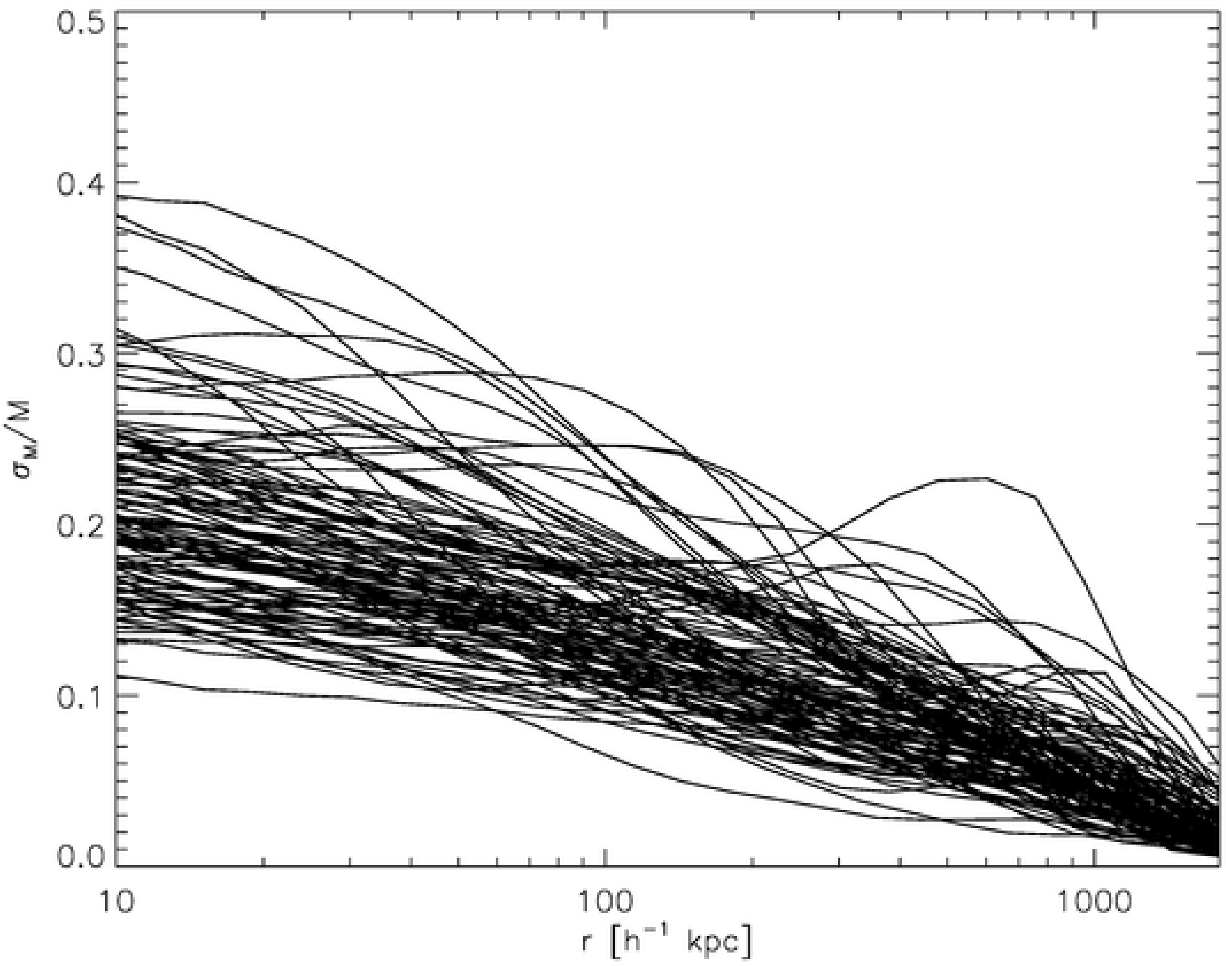

MUSIC-2 simulation by Massimo

20 CLASH clusters in Umetsu+14

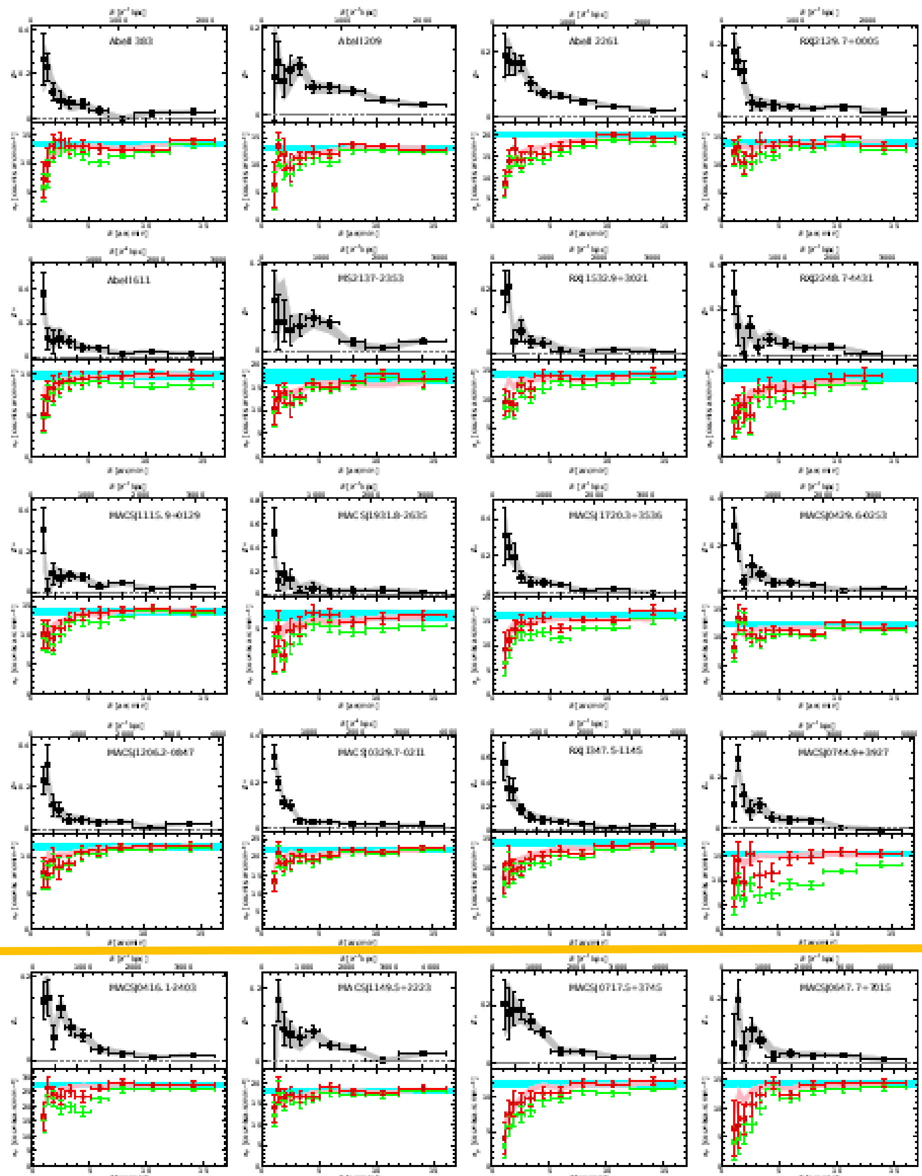

16 X-ray-selected clusters

- 15 clusters from 8.3m Subaru Telescope
- 1 southernmost cluster (RXJ2248) from 2.2m ESO/MPG
- $0.18 < z < 0.69$

$\langle\chi^2/\mathrm{dof}\rangle = 0.92$ for 20 CLASH clusters

4 high-magnification clusters

- All 4 clusters from 8.3m Subaru Telescope

Mass Comparisons @ R=1.5Mpc

Merten+CLASH 14

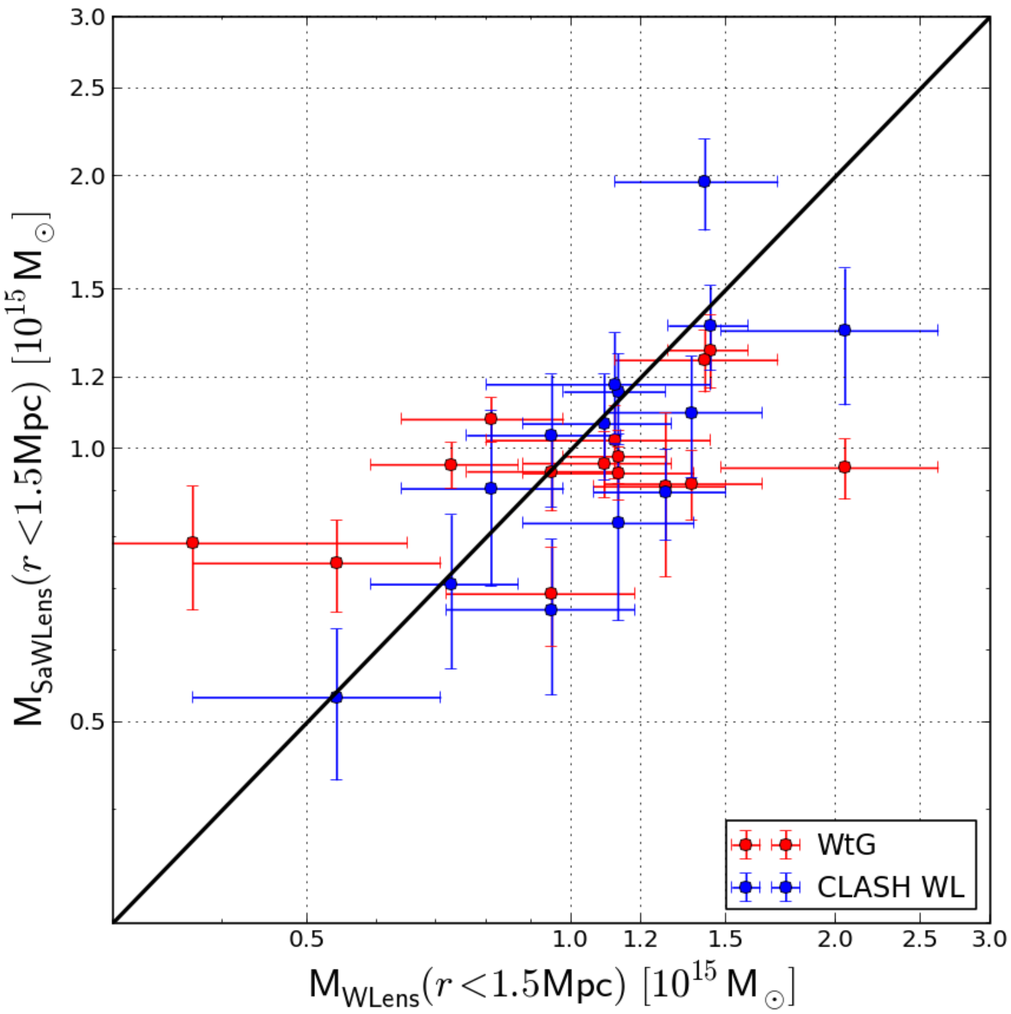

Un-weighted geometric mean mass ratios (<Y/X>=1/<X/Y>)

- <SaWLenS / WL> = 0.96
- <WL / WtG> = 0.91
- <SaWLenS / WtG> = 0.88

WL (Umetsu+14)
→ shear+mag (Subaru)
SaWLenS (Merten+14)
→ SL + shear (HST+Subaru)
WtG (Applegate+14)
→ shear (Subaru)

Note: WL mass calibration uncertainty of 8 percent

Comparison with WtG @R=1.5Mpc

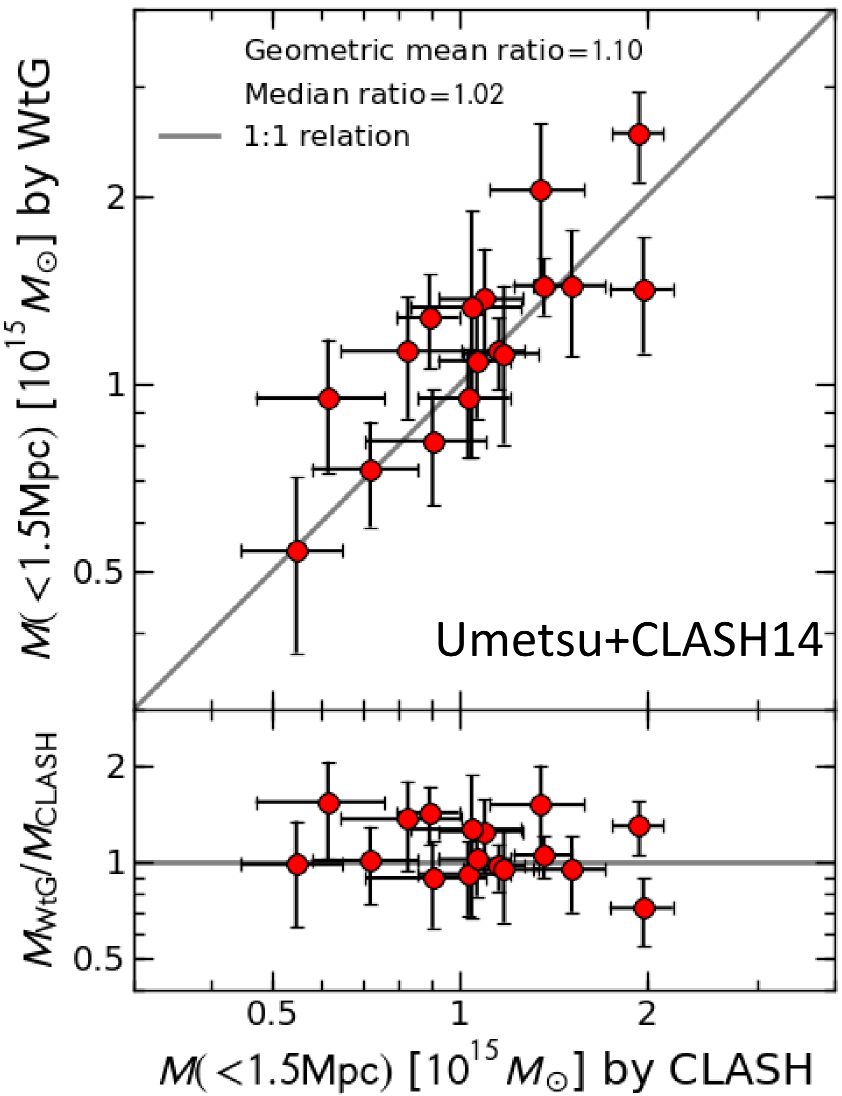

17 clusters in common (Subaru):

- **WtG**: shear-only (Applegate+14), NFW c_{200c}=4 prior
- **CLASH**: shear + magnification, NFW log-uniform: $0.1<c_{200c}<10$

Un-weighted geometric mean mass ratio (<Y/X> = 1/<X/Y>)

- $\langle M_{WtG}/M_{CLASH} \rangle = 1.10$
- Median ratio = 1.02

Systematic uncertainty in the overall mass calibration of 8% from shear-magnification consistency (Umetsu+14)

No mass dependent bias

CLASH Comparisons with X-ray masses

Chandra HSE / Subaru-WL

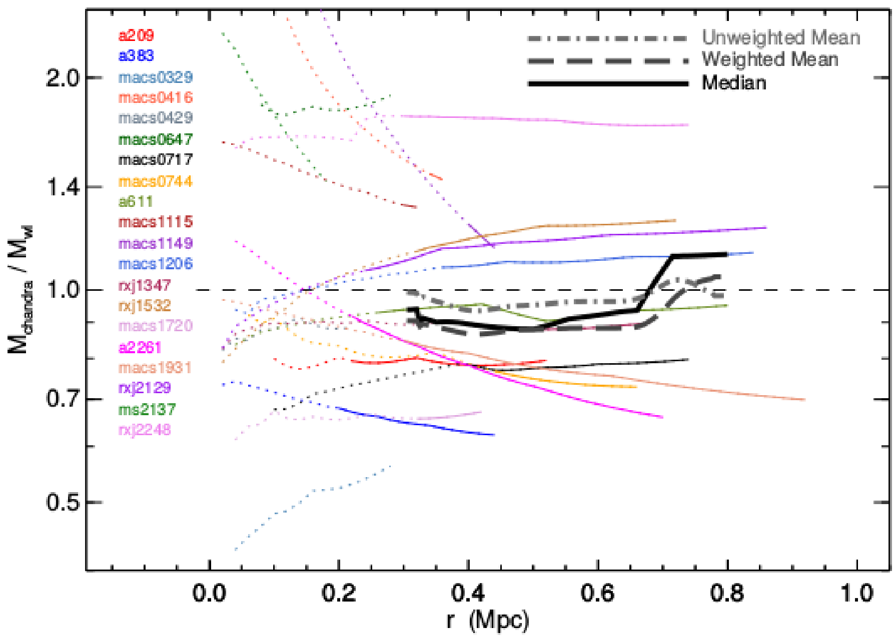

XMM HSE / Subaru-WL

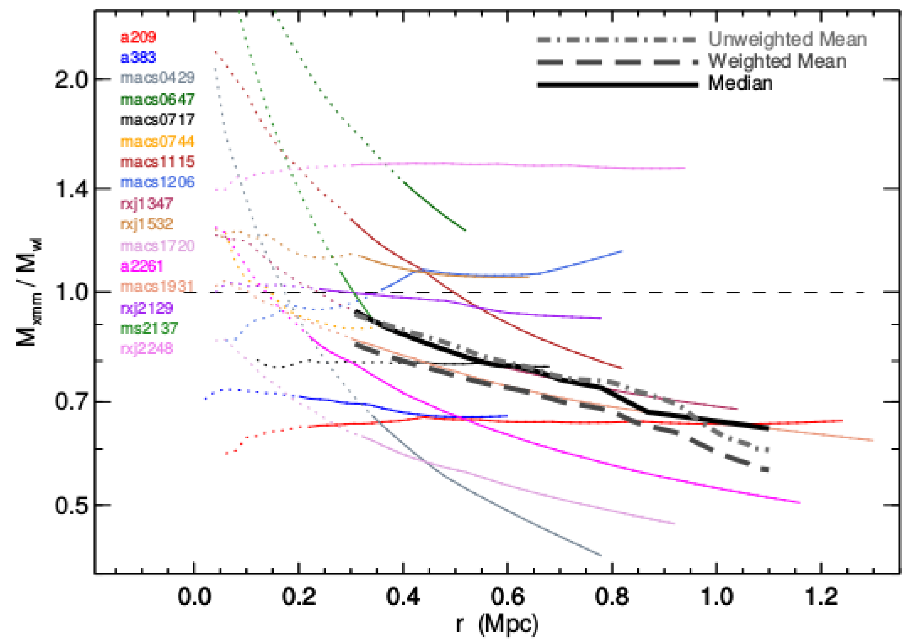

X-ray to WL comparison at R=0.5Mpc

- $b = 1 - \langle M_{\mathrm{Chandra}}/M_{\mathrm{WL}} \rangle = 0.05 \pm 0.07$ (11 clusters)
- $b = 1 - \langle M_{\mathrm{XMM}}/M_{\mathrm{WL}} \rangle = 0.16 \pm 0.06$ (14 clusters)

X-ray to WL comparison at r_{500} [no aperture correction]

- $b = 1 - \langle M_{\mathrm{Chandra}}/M_{\mathrm{WL}} \rangle = 0.09 \pm 0.12$ (20 clusters)
- $b = 1 - \langle M_{\mathrm{XMM}}/M_{\mathrm{WL}} \rangle = 0.41 \pm 0.07$ (16 clusters)

Donahue+CLASH 14, ApJ, accepted (arXiv:1405.7876)
See also Sereno+14

Suzaku-X HSE vs. Subaru WL

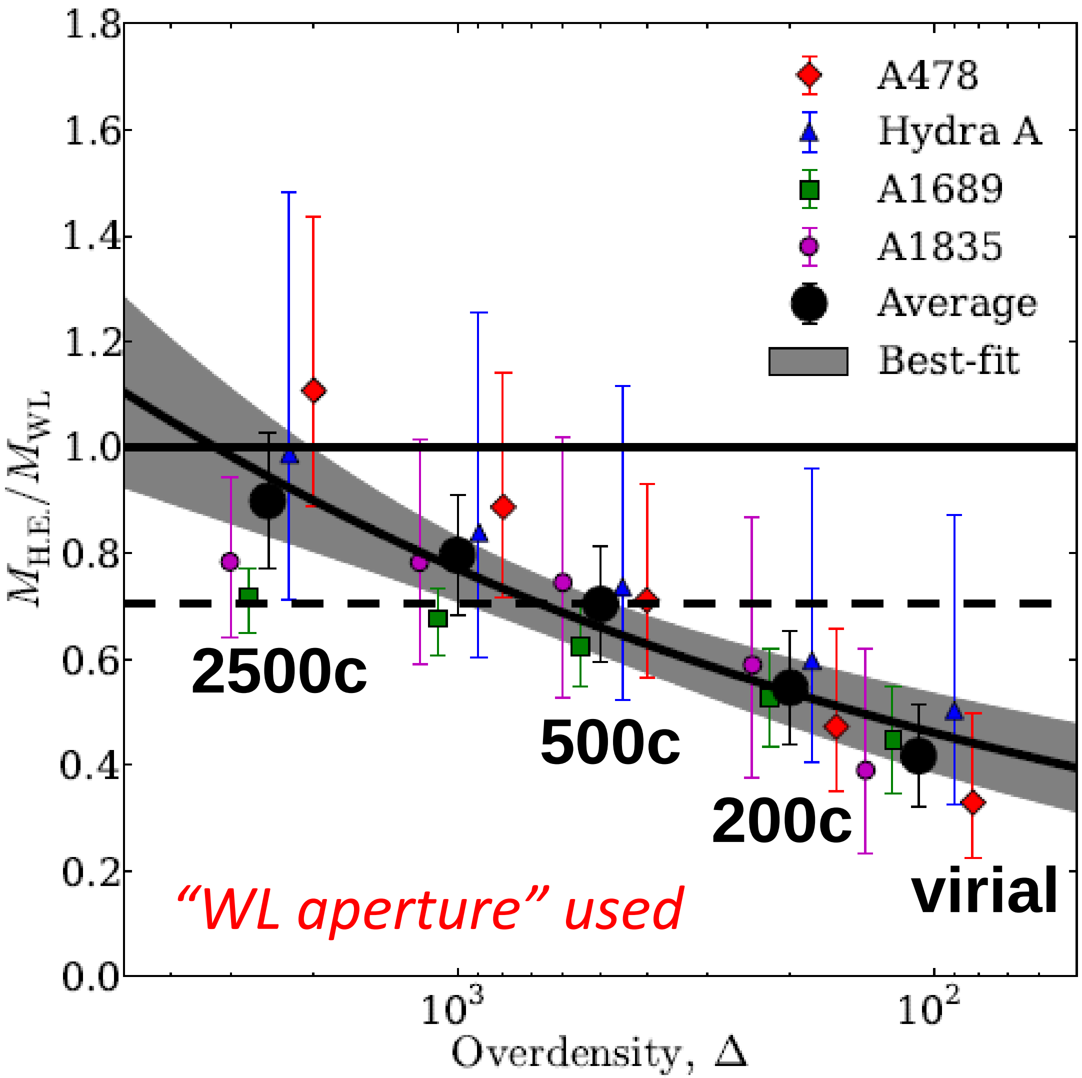

Independent *Suzaku*-HSE vs. Subaru-WL results, consistent with XMM-HSE vs. Subaru-WL of CLASH collaboration

Okabe, Umetsu et al.14, PASJ, in press (arXiv:1406.3451)

Comparison with pre-CLASH results

- **c_{200} vs θ_E relation, consistent with triaxial CDM halos (Oguri+12)**
- **Similar ν (MAH), similar Σ in outskirts (Diemer & Kravtsov 14)**
- **Increased Σ at R<0.5Mpc/h, consistent w orientation bias (Gao+12)**

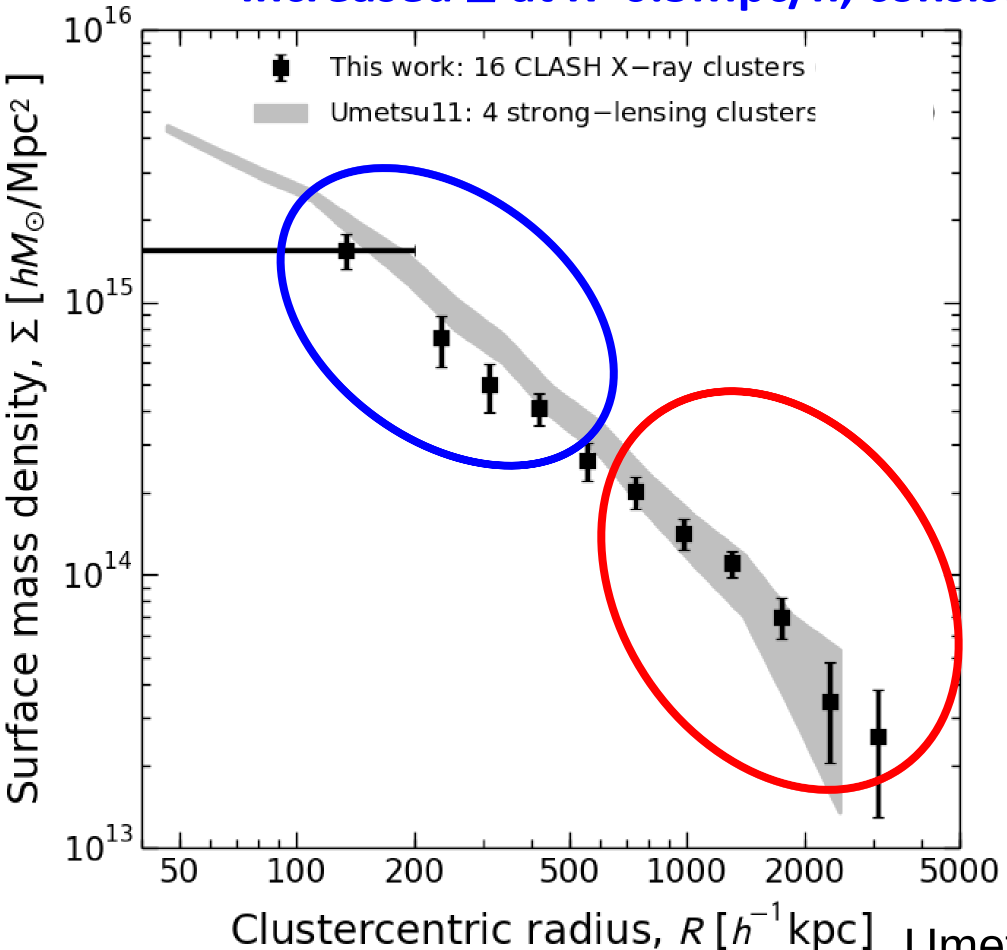

CLASH X-ray-selected sample

- M_{200} = 1.3e15M_{sun}
- c_{200} = 4.0
- θ_E ~ 15" (z_s=2)
- ν=3.8 (b_h~9)

Umetsu11b sample

- M_{200} = 1.7e15M_{sun}
- c_{200} = 6.1
- θ_E ~ 36" (z_s=2)
- ν=4.1 (b_h~11)

Umetsu+14, ApJ, accepted (arXiv:1404.1375)

Shear-Magnification Consistency

M(<r) de-projected assuming spherical NFW (20 CLASH clusters)

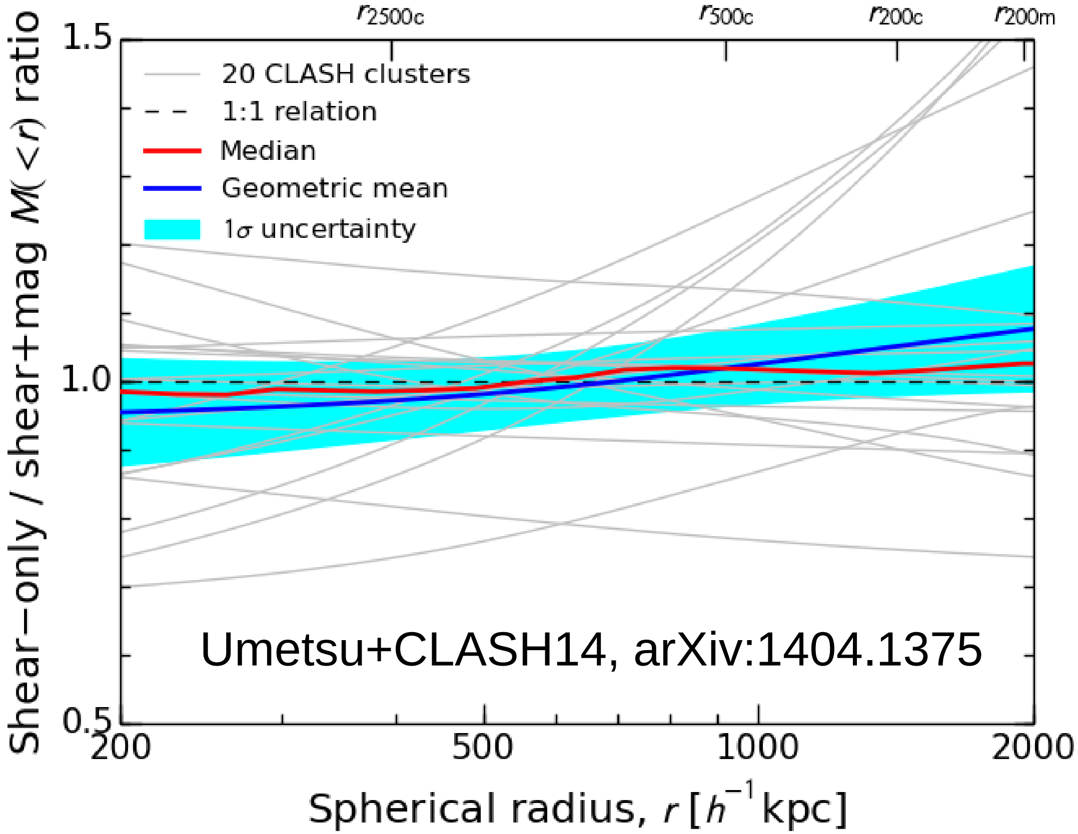

Umetsu et al. 14, ApJ, accepted (arXiv:1404.1375)

Internal systematic uncertainty in the overall mass calibration, empirically derived to be about +/- 8%

Ensemble-averaged DM halo profile

Stacking of weak-lensing signals by weighting individual clusters according to the sensitivity kernel matrix:

$$\langle\langle \widehat{\Delta\Sigma_+} \rangle\rangle = \left(\sum_n \mathcal{W}_{+n} \right)^{-1} \left(\sum_n \mathcal{W}_{+n} \widehat{\Delta\Sigma_{+n}} \right),$$

with the individual sensitivity matrix

$$(\mathcal{W}_{+n})_{ij} \equiv \Sigma_{c,n}^{-2} \left(C_{+n}^{-1} \right)_{ij}$$

defined with the total covariance matrix

$$C_+ = C_+^{\rm stat} + C_+^{\rm sys} + C_+^{\rm lss}.$$

With "trace-approximation", averaging is interpreted as

$$\langle\langle \Sigma_c^{-1} \rangle\rangle = \frac{\sum_n \mathrm{tr}(\mathcal{W}_{+n}) \Sigma_{c,n}^{-1}}{\sum_n \mathrm{tr}(\mathcal{W}_{+n})},$$

CLASH-WL vs. c-M relations

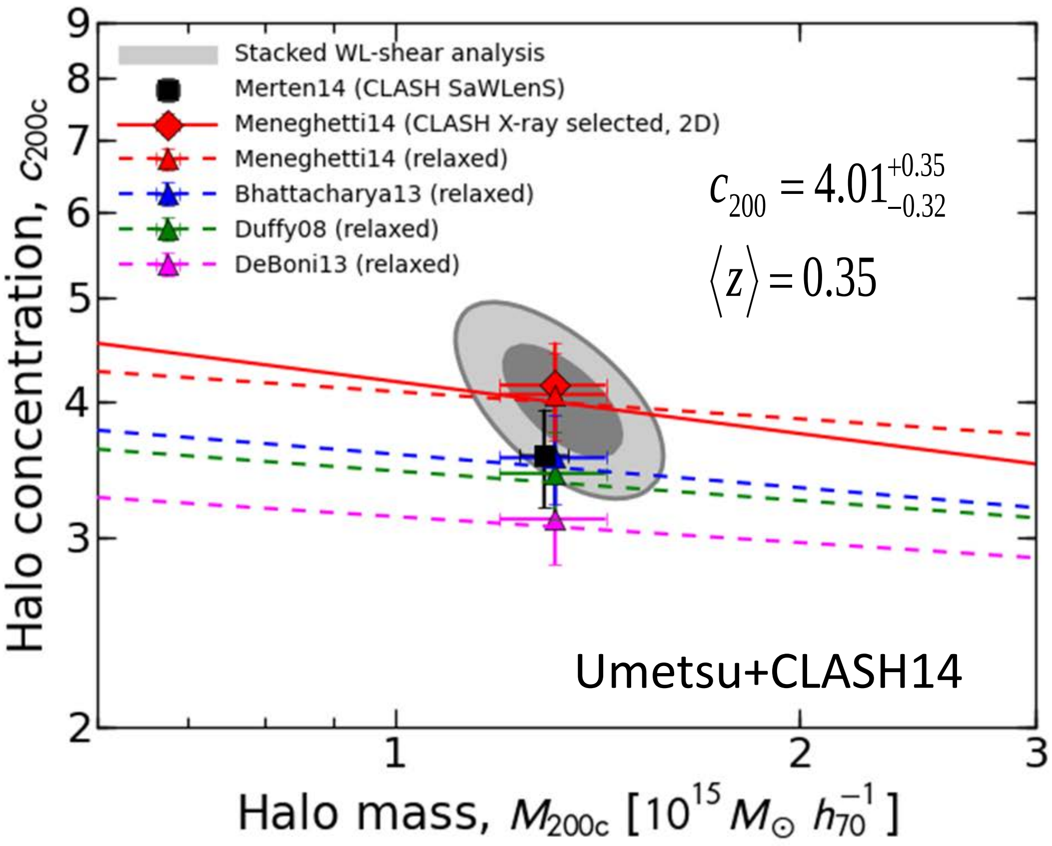

M14 (MUSIC-2): σ_8=0.82
Bhat13: σ_8=0.8
Duffy08: σ_8=0.8
DeBoni13: σ_8=0.78

At low M_{200c}, X-ray selection picks up clusters with higher concentrations (Meneghetti+14)

CLASH: WL vs. X-ray Mass Comparison

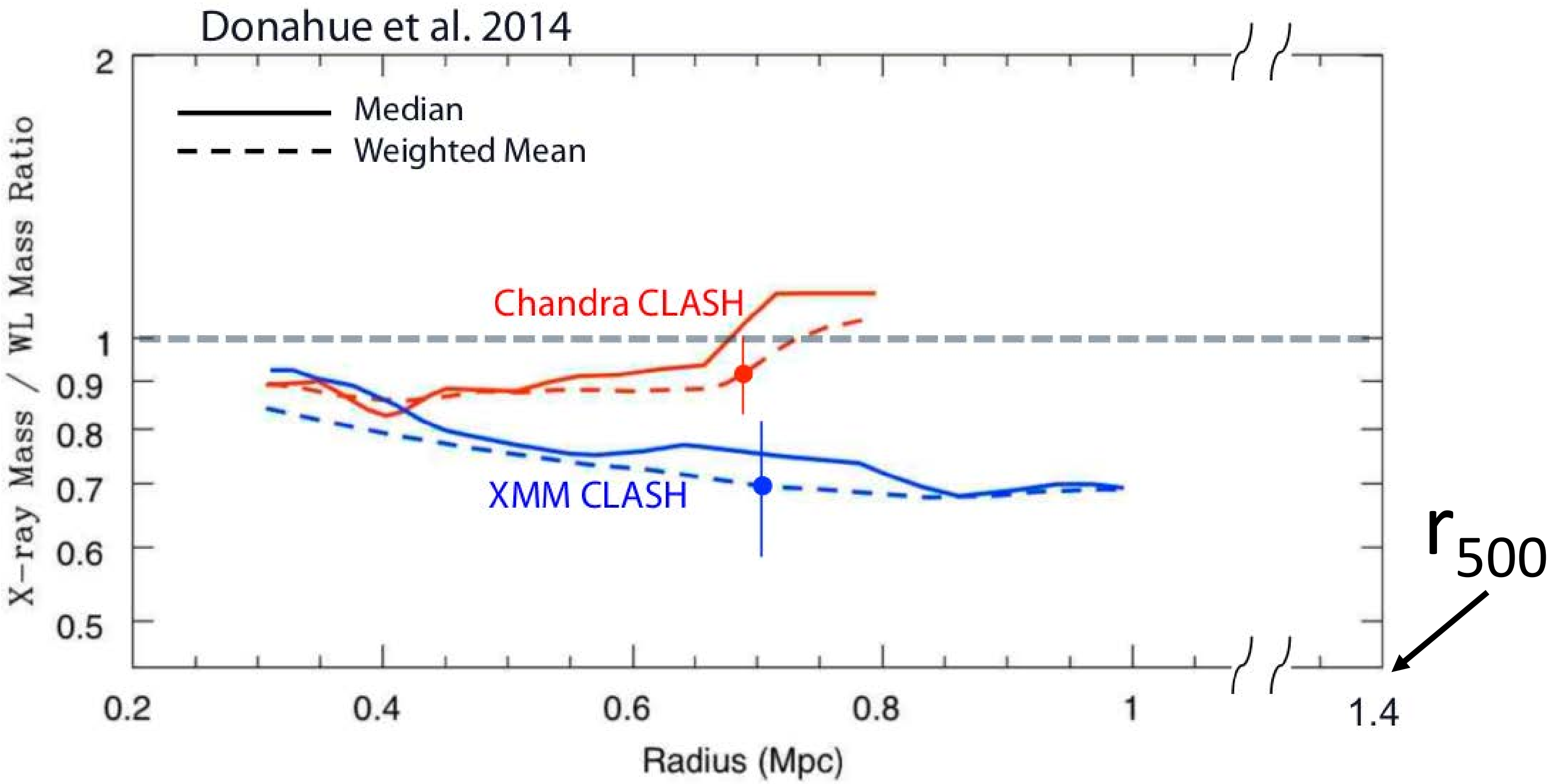

X-ray to WL mass comparison at r_{500}

- $b = 1 - \langle M_{Chandra}/M_{WL} \rangle = 0.22 \pm 0.10$
- $b = 1 - \langle M_{XMM}/M_{WL} \rangle = 0.44 \pm 0.06$

Donahue+CLASH 2014, *ApJ*, 794, 136